國立臺灣師範大學生命科學系碩士論文

青鱂魚仔魚體表離子細胞的排氨參與鈉離子吸收機制

Ammonia-dependent Na^+ uptake in mitochondria-rich cells of medaka (*Oryzias latipes*) larvae

研 究 生：吳 淑 貞

Shu-Chen Wu

指導教授：林 豐 益 博士

Li-Yih Lin

中 華 民 國 九 十 八 年 六 月

Table of Contents

誌　　謝

在重展睽違數年的學生生活前，從未接觸過研究領域的我心情忐忑不安。如今能從無到有、順利畢業，指導教授**林豐益老師**居功闕偉。在研究道路上，老師不時給予鼓勵與指導，放手讓我摸索但適時指引我方向。經常與我們分享自己的歷程，讓我們瞭解所研究事物的價值並自豪之。感謝**黃鵬鵬老師**與**張清風老師**於百忙中在論文及口試上提供寶貴建議。**杜銘章老師**在教學上展現的熱忱及邏輯思維是我為人師的典範。熱心的**童麗珠老師**屢次幫我在慌亂時穩住陣腳。系辦**漢英助教**一再幫忙我這迷糊的研究生補齊口試所需書表，有勞您了。很慶幸我有最好的前導領我走這一段研究生涯。

感謝**廷翰前輩**任勞任怨地到中研院拉針供我揮霍，指導我學習電生理實驗，在我對實驗結果困惑不解時點出癥結，令我豁然開朗。你是個人才，這回我絕不是巴結。感謝**作豪學長**引薦我加入這可愛的 B316 團隊中學習。感謝**仁華前輩**的親切照顧，相信許多同學和我一樣，在妳的幫助下度過迷惘的碩一。**婉婷前輩**總在緊要關頭適時出現，提醒我該完成的事情。B 咖**學弟宗麟**，每天充飽了我下午做實驗所需的滿滿能量。與我一同在陽剛味較重的實驗室中相依為命的**婉萍學妹**，妳和女二舍監成就了我的生活需求，在最後一個學期裡感謝有妳和學弟幫忙準備實驗材料。**咸台**和**家正同學**在分子方面的研究結果，讓我能確定此篇生理研究的意義，雖不熟識，但感謝你們。一同打拼學位的年輕女性們，**惠如**、**翠紋**、**曉蓉**、**于惠**，祝你們未來一切順遂。謝謝**元誠學弟**不時給我鼓勵與小寵物。能在研所期間結交你/妳們這群忘年好友，何其榮幸。

感謝**爸媽**賜予我不俗的基因與完整的栽培，讓我有足夠能力能完成學業。感謝吳家眾姊妹**碧卿**、**瓊梅**、**碧娥**、**宜潔**的體貼與支持，有妳們的地方就有家的感覺。感謝**微波通訊中心侯技士**，不離不棄地照顧我的學生生活，忍受我求學過程中遭遇瓶頸時的脾氣、趕報告時的邋遢，在我幾乎要放棄時鼓勵我堅持，你是我此生的好夥伴。親愛的**惠紋**、**翎斐**、**雅婷**、**敏菁**，雖然現在大家聚少離多，但你們的關懷我銘記在心，我們是永遠的朋友。感謝國立苑高的**麒璋老師**和**祐慈老師**，在我停職進修期間幫忙分擔了我的職務，辛苦你們了。

能得到這麼多熟識或不認識的朋友所施予的無形或有形、直接或間接的幫助，我非常有福，謝謝你們，我愛你們！

吳淑貞

2009 年盛夏

摘　　要

鈉氫交換蛋白(Na^+/H^+ exchanger，NHE)主要分佈於富含粒線體細胞(MR 細胞)頂膜，是淡水魚類鰓上皮執行 Na^+吸收的重要機制，過程中同時發生排酸現象。然而早期文獻從排氨量與 Na^+吸收量呈現相關的結果推論 Na^+吸收過程協同發生排氨，並認為此現象是因 NHE 執行 Na^+/NH_4^+的交換所致。然而近年來發現排氨主要以非離子態 NH_3經由 Rh 蛋白排除，否定了 NHE 執行 Na^+/NH_4^+交換的可能。因此，NHE 如何在淡水環境中驅動 Na^+/H^+交換，及排氨量與 Na^+吸收呈現相關的原因至今仍未明瞭。本研究以青鱂魚仔魚為模式動物，利用掃瞄式離子選擇電極技術(SIET)進行非侵入性量測，探討其體表細胞的 Na^+吸收機制與排 H^+、排 NH_4^+間的關連性，並試圖推論 NHE 如何參與 Na^+吸收機制。結果發現，NHE 抑制劑(100 uM EIPA)浸泡會顯著抑制仔魚排酸、排氨及 Na^+吸收，顯示 NHE 參與此三種離子的調節機制。低鈉水(<0.001 mM)馴養個體會增加體表 Na^+吸收與排 NH_4^+，但降低了體表 H^+濃度；高氨水(5 mM NH_4^+)馴養也造成類似結果。而在測量環境中給予短時間高氨處理(5 mM NH_4^+)可同時抑制排 NH_4^+與 Na^+吸收並增加體表 H^+累積濃度。以上結果顯示魚體排氨機制可能驅動 NHE 進行 Na^+吸收。從仔魚體表單一細胞離子流測量結果發現，Na^+吸收與排 NH_4^+主要發生在 MR 細胞。以 H^+電極測量後發現體表 MR 細胞有排酸(MRC^+)和排鹼(MRC^-)二型，高氨與與低鈉水馴養都會增加 MRC^-的比例。在測量環境中給予短時間高氨處理(5 mM NH_4^+)，排鹼型 MR 細胞會轉變為排酸型，而同時抑制 Na^+吸收。顯示 MRC^-可能排除大量 NH_3造成細胞外 H^+被結合成 NH_4^+而形成排鹼現象。此外，酸性水體(pH6)理論上不利於 NHE 的驅動，然而結果顯示短期酸處理促進 Na^+吸收與排 NH_4^+。由此推論 Rh 蛋白在輔助 NH_3排放的過程中，會造成細胞膜內外 H^+梯度的增加進而有利推動 NHE 進行 Na^+吸收。

Abstract

The mechanisms of Na^+ uptake and NH_4^+ excretion at gills of freshwater fish have been studied for decades but the detail remains unclear. To investigate the mechanisms, a scanning ion-selective electrode technique (SIET) was applied to detect the H^+, Na^+, and NH_4^+ activities and fluxes at the skin surface of newly-hatched medaka larvae. By probing the ionic fluxes at specific cells in the skin, MRCs were found to be the major sites for Na^+ uptake and NH_4^+ excretion. However, H^+ probing at MRCs revealed two groups of MRCs: acid-secreting MRCs (MRC^+) and base-secreting (probably NH_3) MRCs (MRC^-). Treatment with EIPA (100 μM) respectively blocked H^+ excretion, NH_4^+ excretion, and Na^+ uptake by 22%, 35%, and 54 %, suggesting that the Na^+/H^+ exchanger (NHE) is involved in H^+, Na^+, and NH_4^+ transport. Low-Na^+ water (< 0.001 mM) or high-NH_4^+ water (5 mM) acclimation caused more MRC^- appearing in skin surface, and simultaneously increased Na^+ uptake and NH_4^+ excretion but decreased or even reversed the H^+ gradient at the skin and the H^+ flux at MRCs. Raising the external NH_4^+ significantly blocked NH_4^+ excretion and Na^+ uptake, but increased the H^+ gradient at the skin. In contrast, raising the acidity of the water (pH 7 to pH 6) enhanced NH_4^+ excretion and Na^+ uptake by MRCs while the H^+ activity at the apical surface of MRCs was reduced. The correlation between NH_4^+ production and H^+ consumption suggests that MRCs excrete non-ionic NH_3 (base) by an acid-trapping mechanism. The present study suggests a Na^+/NH_4^+ exchange pathway in apical membranes of MRCs, in which a coupled NHE and Rhesus (Rh) glycoprotein is involved, and the Rh glycoprotein may drive the NHE by generating H^+ gradients across apical membranes of MRCs.

Introduction

Na^+/NH_4^+ exchange in fish gills

Freshwater (FW) fishes are subject to passive loss of salts in hypotonic environments. To compensate the ionic loss, FW fishes actively take up Na^+ and Cl^- from the dilute environment by their gills (Randall et al., 2002). In 1939, August Krogh pioneered the study of Na^+/Cl^- uptake in FW fishes and suggested that blood ions such as NH_4^+ and HCO_3^- are exchanged for Na^+ and Cl^- respectively at fish gills. Since then, many studies have been carried out to investigate the mechanisms involved in Na^+ uptake and NH_4^+ excretion. Shaw (1960) and Maetz and Garcia Romeu (1964) were the first to provide evidence supporting NH_4^+ exchange for Na^+. Thereafter, several studies also reported that the amount of NH_4^+ excreted is close to the amount of Na^+ taken up in intact salmonids or in isolated head preparations (McDonald and Millsgan, 1988; Payan, 1978; Salama et al., 1999; Wright and Wood, 1985). In addition, NH_4^+ loading was found to stimulate Na^+ uptake (Kerstetter and Keeler, 1976; Salama et al., 1999; Wilson et al., 1994). These observations supported the presence of a Na^+/NH_4^+ exchange mechanism in fish gills.

However, Kerstetter and colleagues (1970) found that increased Na^+ uptake was not correlated to NH_4^+ excretion but to H^+ excretion and proposed that Na^+ is in fact exchanged for H^+. This Na^+/H^+ exchange mechanism was also proposed earlier on frog skin by Romeu et al. (1969) who found a 1:1 relationship between net Na^+ influx and net H^+ efflux. Meantime, subsequent studies also suggested that non-ionic diffusion of NH_3 plays a major role in ammonia excretion and NH_4^+ excretion is at best only loosely coupled to Na^+ uptake (Kirschner et al., 1973; Wilkie and Wood, 1994; Wilson et al., 1994;

Wright et al., 1989). A Na^+/H^+ exchanger (NHE) was further suggested to be a player in Na^+/H^+ exchange based on the inhibition of Na^+ uptake by amiloride. However, amiloride was also reported to cause a reduction in ammonia excretion in several studies (Payan, 1978; Randall et al., 1999; Wilson et al., 1994), thus NH_4^+ was suggested to replace H^+ on the NHE and exchange for Na^+ (Wilkie, 2002). Therefore whether Na^+ uptake is through Na^+/ NH_4^+ or Na^+/H^+ exchange mechanism remains controversial.

Role of NHE in Na^+ uptake

The NHEs are electroneutral transporters that catalyze exchanges of Na^+ and H^+ whose functions are affected by intra- and extracellular ion concentrations (Parks et al., 2008). Nine isoforms (SLC9A1-9) have been identified in the human genome. Among them, NHE2 and NHE3 are expressed in the apical membranes of gastrointestinal and renal cells, and are suggested involving in systemic Na^+ uptake and H^+ excretion of mammalians (Choe et al., 2005). Those two NHE isoforms could be predicted from genome database of fishes. The branchial NHE of fishes was first cloned from the Japanese Osorezan dace (*Tribolodon hakonensis*), which lives in an acidic lake of pH 3.5 (Hirata et al., 2003). The NHE3 of Osorezan dace located in the apical membranes of mitochondria-rich cells and the mRNA expression of NHE3 was induced in such extremely acidic lake which is theoretically disfavoring NHE function (Hirata et al., 2003). Recently, Yan et al. (2007) cloned and identified zNHE3 in H^+-pump-rich cells (HRCs) of zebrafish gills. Low-Na^+ (L-Na) acclimation increased the mRNA expression of zNHE3 but suppressed that of H^+-ATPase. Ivanis et al. (2008) used homologous antibodies to localize NHE2/NHE3 in the apical membranes of MRCs in rainbow trout

(*Oncorhynchus mykiss*). In tilapia (*Oreochromis mossambicus*), a homologous antibody was also labeled NHE3 in the apical membrane of a subtype of MRCs (Inokuchi et al., 2008). Those studies suggested that the apically located NHEs play a significant role in Na^+ uptake in FW fishes. Although the accumulating evidence of NHE has been proposed (Evans et al., 2005; Hwang and Lee, 2007), the driving force of apical NHE in FW fishes remains a question. In common fresh water, the Na^+ is too few and the blood-to-water pH gradient is not large enough to favor driving of the apical NHEs to take up Na^+ (Parks et al., 2008).

Role of H^+-ATPase in Na^+ uptake

An alternative pathway for the Na^+/H^+ exchange mechanism was proposed by Avella and Bornancin (1989). They suggested that NHE could not function in Na^+ uptake in fishes living in extremely dilute environments, and recommended that an apical v-type H^+-ATPase electrochemically linked to an epithelial Na^+ channel (ENaC) drives Na^+ uptake from fresh water. The two pathways through an NHE or H^+-ATPase-coupled ENaC have become the current dominant models for Na^+ uptake in FW fish (Evans et al., 2005). Pharmacological studies reported that the H^+-ATPase-specific inhibitor, bafilomycin, greatly impaired Na^+ uptake in tilapia, carp (Fenwick et al., 1999), rainbow trout (Bury and Wood, 1999), and soft-water acclimated zebrafish (Boisen et al., 2003). Recent studies combining molecular and physiological methods provided more convincing evidence for the role of H^+-ATPase in Na^+ uptake. In trout, two groups of isolated branchial MRCs, PNA^+ and PNA^- MRCs were discriminated by peanut lectin agglutinin (PNA). Hypercapnic acidosis increased H^+-ATPase expression on PNA^- MRCs only (Galvez et al.,

2002), and bafilomycin-sensitive acid-activated $^{22}Na^+$ uptake was observed in PNA^- MRCs only (Reid et al., 2003). In zebrafish larvae, H^+-ATPase was identified locating in a subtype of MRCs, HRCs, which showed a higher H^+ flux than other skin cells (Lin et al., 2006). Knockdown of H^+-ATPase expression reduced H^+ excretion and Na^+ uptake in zebrafish (Horng et al., 2007). The accumulation of Sodium Green, a Na^+ indicator, was observed in HRCs and was inhibited by bafilomycin (Esaki et al., 2007). All these studies suggest that H^+-ATPase is involved in Na^+ uptake. In addition, phenamil (a specific inhibitor for ENaC) decreased the $^{22}Na^+$ uptake and the intracellular pH in isolated PNA^- MRCs of trout (Parks et al., 2007) demonstrated the co-working between H^+-ATPase and ENaC. By using a human polyclonal antibody, the ENaC-like protein was shown to be located in branchial MRCs and/or PVC in tilapia and rainbow trout (Wilson et al., 2000). However, the specificity of the ENaC antibody has been debated because the cloning of Na^+ channel has never been successful in fishes (Hwang and Lee, 2007). Therefore the mechanism of H^+-ATPase/ENaC in Na^+ uptake is still controversial.

Role of Rhesus glycoproteins in NH_3/NH_4^+ excretion

Kerstetter and Keeler (1976) suggested that Na^+/NH_4^+ exchange might occur through the NHE, hence the NH_4^+ gradient could drive the branchial Na^+ uptake. However, some features in those studies supporting Na^+/NH_4^+ exchange mechanism are against the involvement of NHE in NH_4^+ excretion: the stoichiometric relationship between the ammonia efflux and Na^+ influx in most cases is not 1:1; the pattern of ammonia efflux has never exhibited saturation kinetics in any study; ammonia still can be excreted in fish transferred to Na^+-poor water (Wilkie, 1997). Ammonia excretion may be

achieved in other predominant mechanism, such as diffusion, than through the NHE.

It is well understood that FW fishes have deep tight junctions to minimize ion loss through paracellular pathway, ionic NH_4^+ is unlikely to diffuse across the relatively impermeable gill epithelium. Kerstetter et al. (1970) suggested that non-ionic NH_3 diffusion plays a big part in branchial ammonia excretion. As mentioned in above paragraph, the subsequent studies also indicated that non-ionic NH_3 is the major form of ammonia excreted by gills through an "acid-trapping" mechanism (Kirschner et al., 1973; Wilkie and Wood, 1994; Wilson et al., 1994; Wright et al., 1989). It is suggested that NH_4^+ (the major form of ammonia in blood) dissociates into H^+ and NH_3, the latter diffuses across gill epithelium and trapped by external H^+, maintaining a blood-to-water NH_3 gradient favorable for continuously NH_3 excretion (Wilkie, 1997).

Recently, studies on Rhesus glycoproteins (Rh proteins) suggested that Rh proteins are ammonia transporters, which function as NH_3 channels for NH_3/NH_4^+ excretion (Khademi et al., 2004; Winkler, 2006). Several isoforms of Rh proteins (Rhag, Rhbg, Rhcg1, and Rhcg2) were also identified from fish gills (Braun et al., 2009; Hung et al., 2007; Nakada et al., 2007a; Nakada et al., 2007b; Nawata et al., 2007). Using a zebrafish model and morpholino gene knockdown, Shih and colleagues demonstrated that the apical isoform, Rhcg1, is involved in ammonia excretion by HRCs, and also suggested that H^+-ATPase generates an acidic layer to drive non-ionic NH_3 diffusion through Rhcg1 (Shih et al., 2008). That was the first loss-of-function study of Rh proteins conducted in intact animal. Thereafter, a similar conclusion was also reported in renal ammonia excretion of mammalian by investigating Rhcg knockout mice (Biver et al., 2008). The findings that Rh proteins mediated ammonia excretion

apparently consolidated the acid-trapping mechanism of NH_3 excretion.

Evidence for Na^+ uptake and NH_4^+ excretion by MRCs

Earlier studies on branchial Na^+ transport usually measured the $^{22}Na^+$ flux in a whole animal or an isolated fish head, which provides only Na^+ flux of a whole animal or gills. The isolation of head is an invasive preparation and usually causes unexpected influences. The former approaches could not provide direct evidence for the role of MRCs in Na^+ uptake or NH_4^+ excretion. MRCs are now accepted to be the major sites for Na^+ uptake based on the localization of NHE and H^+-ATPase mRNA or protein in MRCs (Hwang and Lee, 2007). Recently, new methods by measuring $^{22}Na^+$ influx of isolated branchial cells (Reid et al., 2003) and Sodium Green accumulation in MRCs of intact zebrafish embryos (Esaki et al., 2007; Flynt et al., 2009) provided evidence for Na^+ uptake in MRCs. However, those methods still could not provide sequential (temporal) information or quantity of Na^+ uptake by individual MRCs.

Lin et al. (2006) established an *in vivo* zebrafish model which combines electrophysiological (scanning ion-selective electrode technique (SIET)) and molecular approaches to demonstrate that a novel H^+-pump-rich cell (HRC) in gills and embryonic skin is an acid-secreting cell. Subsequent studies further suggested that Na^+ uptake is mediated by HRCs (Esaki et al., 2007; Horng et al., 2007), and NHE3 is indentified in the apical membrane of HRCs (Yan et al., 2007). Meanwhile, Rhcg1 was identified in the apical membrane of HRCs (Nakada et al., 2007a) and suggested to be involved in NH_3 excretion of zebrafish larvae (Shih et al., 2008). The presence of Na^+ uptake and NH_4^+ excretion in the same cell (HRCs) of zebrafish led us to reconsider other

possible mechanisms for Na^+/NH_4^+ exchange. Lately, Tsui and colleagues (2009) examined the same question using cultured trout gill epithelium and suggested that Na^+/NH_4^+ exchange is mediated by a putative protein complex including an Rh protein, the NHE, H^+-ATPase, and an unidentified Na^+ channel. However, it is still a premature model and needs more-direct evidence to support it. To answer this question, we used the SIET to detect Na^+ uptake by HRCs of zebrafish larvae and tried to figure out if Na^+/NH_4^+ exchange occurs in HRCs. However, we found that the Na^+ current detected at HRCs was too small to conduct functional assays. Alternatively, we detected a significant Na^+ influx at MRCs of another model fish, Japanese medaka (*Oryzias latipes*). Therefore, we established a new medaka model in this study to examine the mechanism of Na^+ uptake and NH_4^+ excretion.

Purpose

In this study, we hypothesized that the NHE is involved in Na^+ uptake, and the process of Na^+ uptake is dependent on NH_4^+/NH_3 excretion. Using the non-invasive technique, SIET, we attempted to examine the relation between Na^+ uptake and NH_4^+ excretion by specific cells of madaka larvae, and provide convincing evidence for the function of Na^+ uptake in MRCs. In addition, we tried to determine a possible mechanism for Na^+ and NH_4^+ transport. Our specific aims were:

1. To demonstrate Na^+ uptake and NH_4^+ excretion by individual MRCs.
2. To examine if Na^+/NH_4^+ exchange occurs in MRCs.
3. Using an inhibitor (EIPA) to examine if NHE is involved in Na^+/NH_4^+ exchange.
4. To find out a possible mechanism for Na^+/NH_4^+ exchange.

Materials and Methods

Experimental animals (medaka larvae)

Mature medaka (*Oryzias latipes*, obtained from Institute of Cellar and Organismic Biology, Academia Sinica, Taipei) were reared in circulating tap water at 27 ℃ with a photoperiod of 14 h of light/12 h of dark. The females spawned from the start of the light period every day. Fertilized egg clusters were collected from the belly of females and rinsed with running tap water to remove the sludge and separate the clusters into single eggs. The eggs were incubated in normal water (see below) for the first two days then sorted into different acclimation groups and incubated in different artificial fresh waters for five more days, incubation solution was replenish daily during the cultured period. Embryos usually hatched at the end of the incubation, and 7 days post-fertilization (dpf) larvae were used for the subsequent experiments.

Incubation solutions for acclimation

All incubation solutions were prepared by adding various salts (Sigma-Aldrich, St. Louis, MO, USA) to the re-distilled water (Milli-RO60; Millipore, USA). The normal water (NW) contained (in mM) 0.5 NaCl, 0.2 $CaSO_4$, 0.2 $MgSO_4$, 0.16 KH_2PO_4, and 0.16 K_2HPO_4 (pH7.0). The low-Na^+ water (L-Na) contained 0.25 $MgCl_2$, 0.2 $CaSO_4$, 0.16 KH_2PO_4, and 0.16 K_2HPO_4 (pH6.8). The high-NH_4^+ (H-Amm) water was prepared by adding 2.5 mM $(NH_4)_2SO_4$ to NW. No significant delay in hatching was founding in larvae acclimated to L-Na or H-Amm water.

Scanning ion-selective electrode technique (SIET)

The SIET was used to measure H^+, Na^+, and NH_4^+ activities and fluxes at the surface of medaka larvae. Glass capillary tubes (no. TW 150-4, World Precision Instruments, Sarasota, FL, USA) were pulled on a Sutter P-97 Flaming Brown pipette puller (Sutter Instruments, San Rafael, CA, USA) into micropipettes with tip diameters of 3~4 μm. These were then baked at 120 ℃ overnight and vapor-sianized with dimethyl chlorosilane (Sigma-Aldrich) for 30 min. The micropipettes were backfilled with a 1-cm column of electrolytes and frontloaded with a 20- to 30-μm column of liquid ion exchanger cocktail (Sigma-Aldrich) to create an ion-selective microelectrode (probe). The following ionophore cocktails and electrolytes (in parentheses) were used: H^+ ionophore I cocktail B (40 mM KH_2PO_4, and 15 mM K_2HPO_4); Na^+ ionophore II cocktail A (100 mM NaCl); and NH_4^+ ionophore I cocktail B (100 mM NH_4Cl). The details of the system were described in previous reports (Lin et al., 2006; Smith et al., 1999). To calibrate the ion-selective probe, the Nernstian property of each microelectrode was measured by placing the microelectrode in a series of standard solutions (pH 6, 7, and 8 for the H^+ probe; 1, 10, and 100 mM NaCl for the Na^+ probe; 0.1, 1,and 10 mM NH_4Cl for the NH_4^+ probe). By plotting the voltage output of the probe against log $[H^+]$, $[Na^+]$, and $[NH_4^+]$ values, a linear regression yielded a Nernstian slope of 58.6 ± 0.6 (n = 10) for H^+, 57 ± 0.3 (n = 10) for Na^+, and 58.2 ± 0.8 (n = 10) for NH_4^+.

Measurement and definition of surface ionic gradient

The SIET was performed at room temperature (26~28℃) in a small plastic recording chamber filled with 2 ml of "recording medium" that contained NW, 300 μM MOPS buffer (Sigma-Aldrich), and 0.3 mg/l ethyl 3-aminobenzoate methanesulfonate (MS-222, Sigma-Aldrich), the pH of recording media was

adjusted to 7.0 by adding 1N NaOH or 1N HCl. Before the measurement, an anesthetized larva was positioned in the center of the chamber with its lateral side contacting the base of the chamber. The ion-selective probe was moved to the target position (10~20 μm away from the larval surface) to record the ionic activities, then the probe was moved away (~10 mm) to record the background. In this study, $\Delta[H^+]$, $\Delta[Na^+]$, and $\Delta[NH_4^+]$ were respectively used to represent the measured H^+, Na^+, and NH_4^+ gradients between the targets (at surface of larval skin) and background. The selectivity coefficients of the Fluka NH_4^+ ionophore I cocktail B is only four times more selective for NH_4^+ than for K^+. Therefore we used "K^+-free recording medium" ((in mM) 0.5 NaCl, 0.05 $(NH_4)_2SO_4$, 0.2 $CaSO_4$, 0.2 $MgSO_4$, 0.16 NaH_2PO_4, and 0.16 Na_2HPO_4) for NH_4^+ probing to avoid K^+ interfering.

Measurement and calculation of cellular ionic flux

An anesthetized larva was laid laterally in the chamber for SIET measurements. Under the differential interference contrast (DIC) microscope, the apical membranes of MRCs in larval skin could be identified (Fig. 4A). The microelectrode was moved to a position about 2 μm above the apical surface of the cells. At every position, the voltage difference in microvolts was measured by probing orthogonally to the surface at 10-μm intervals. The "single-spot recording" was performed at the surface of an MRC or a keratinocyte (KC) for about 10 replicates, and the median of the repeats was used for calculating the ionic flux of the cell. In addition, a "line-scan recording" was made by probing a series of spots along a line (40 μm with nine spots) across the surface of MRCs and adjacent KCs. At every spot, the voltage difference in microvolts was measured by probing orthogonally to the surface at a 10-μm distance.

The calculation of ionic flux was shown in previous reports (Donini and O'Donnell, 2005; Shih et al., 2008; Smith et al., 1999). Voltage differences obtained from the ASET software were converted into concentration (activity) gradients using the following equation:

$$\Delta C = C_b \times 10^{(\Delta V / S)} - C_b; \quad (1)$$

where ΔC (μmole l^{-1} cm^{-3}) is the concentration gradient between the two points; C_b (μmole l^{-1}) is the background ion concentration; Δ*V* (μV) is the voltage gradient obtained from ASET; and *S* is the Nerst slope of the electrode. The concentration gradient was subsequently converted into ionic flux using Fick's law of diffusion in the following equation:

$$J = D(\Delta C) / \Delta X; \quad (2)$$

where *J* (pmole cm^{-2} s^{-1}) is the net flux of the ion; *D* is the diffusion coefficient of the ion (9.37×10^{-5} cm^2 s^{-1} for H^+; 1.55×10^{-5} cm^2 s^{-1} for Na^+; and 2.09×10^{-5} cm^2 s^{-1} for NH_4^+); ΔC (pmole l^{-1} cm^{-3}) is the concentration gradient; and Δ*X* (cm) is the distance between the two points.

Treatment with 5-ethylisopropyl amiloride

The 5-ethylisopropyl amiloride (EIPA, Sigma-Aldrich) were dissolved in dimethyl sulfoxide (DMSO, Sigma-Aldrich) and diluted with acclimation water. The experimental larvae were incubated in acclimation water with final concentration of 10, 100, or 1000 μM EIPA (DMSO:acclimation water = 1:1000) for 10 min while the controls were incubated in acclimation water with 1/1000 DMSO for 10 min. After treatment, EIPA was washed off immediately and the larvae were placed in recording medium then measured with the SIET.

Illustrations of Experimental Designs

Samples preparation :

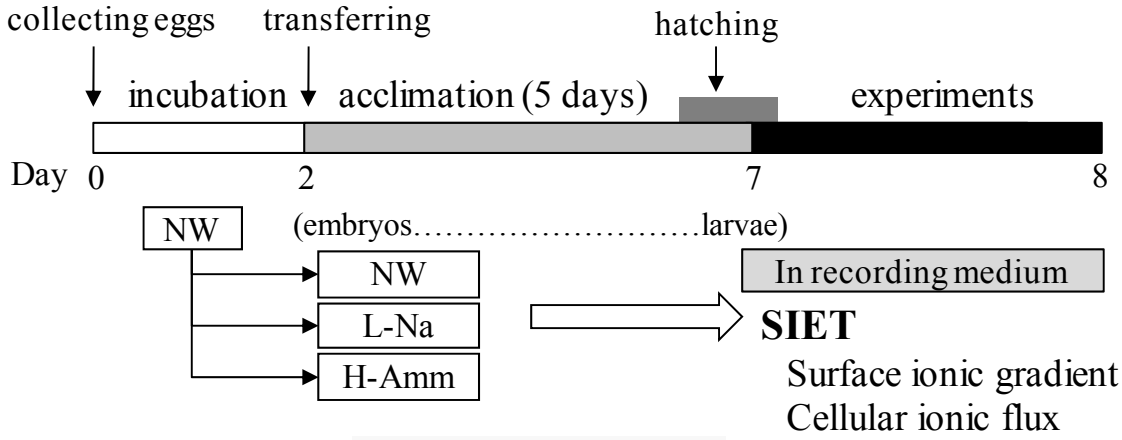

Experiment 1.

Na^+, H^+, and NH_4^+ gradients at the skin of medaka larvae.

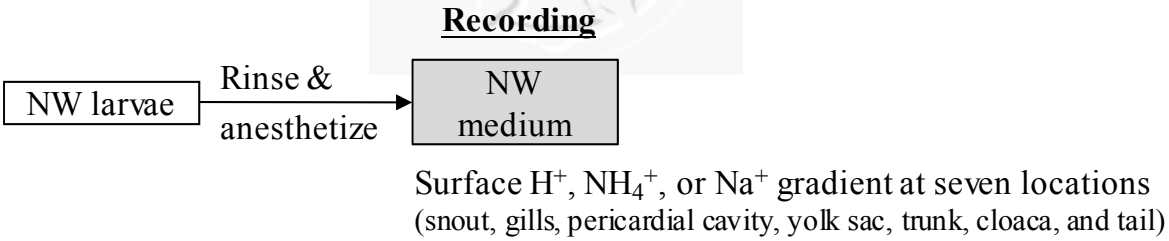

Experiment 2.

Na^+, H^+, and NH_4^+ gradients in larvae acclimated to L-Na water.

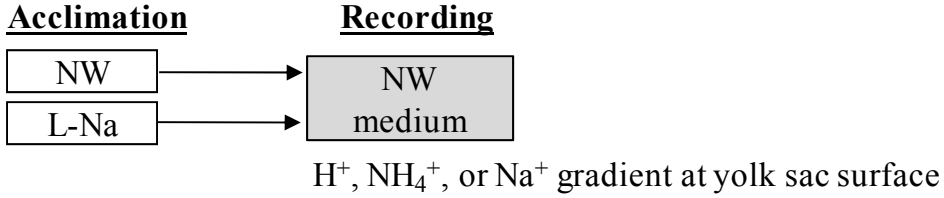

Experiment 3.

Effects of EIPA on ionic gradients.

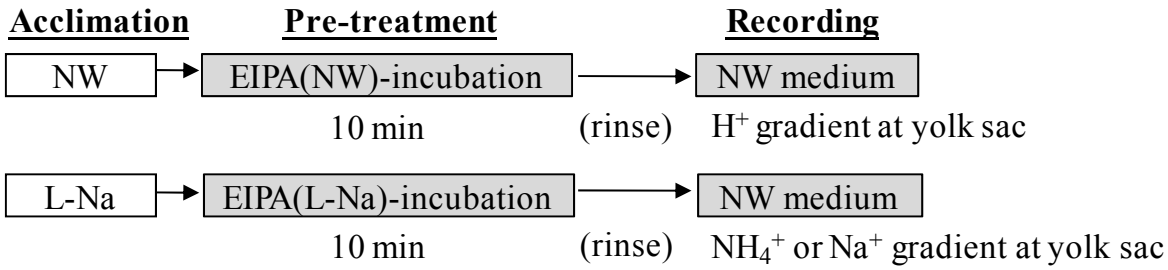

Experiment 4.

Na^+, H^+, and NH_4^+ fluxes at MRCs and KCs.

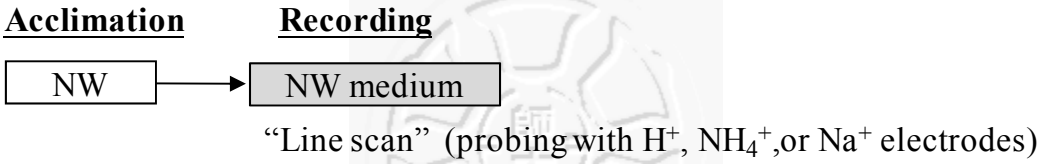

Experiment 5.

H^+, Na^+, and NH_4^+ fluxes at MRCs and KCs in larvae acclimated to L-Na or H-Amm.

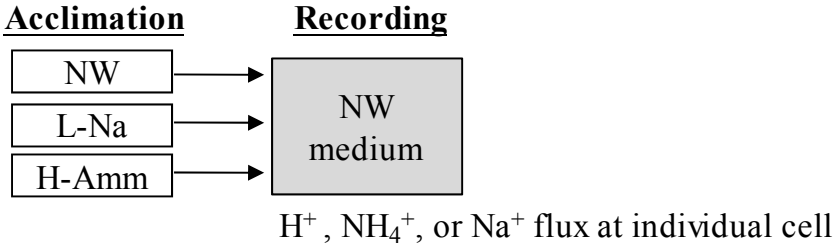

Experiment 6.

Acute effects of external H-Amm on ionic gradients.

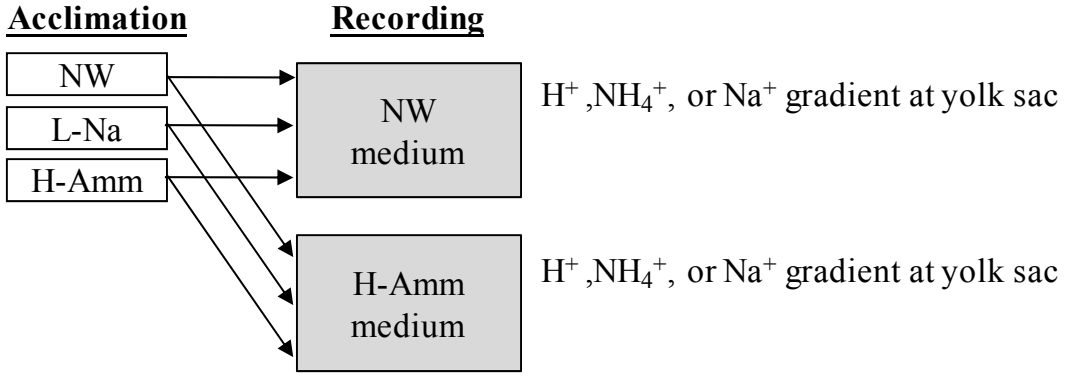

Experiment 7.

Acute effects of external H-Amm on ionic fluxes at specific cells.

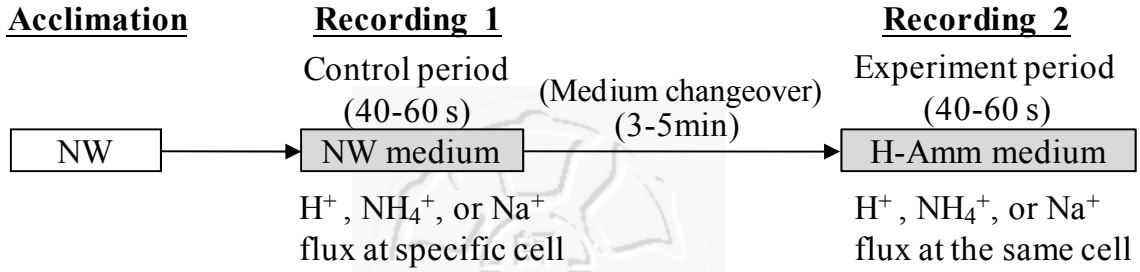

Experiment 8.

Acute effects of the external pH on ionic gradients and fluxes.

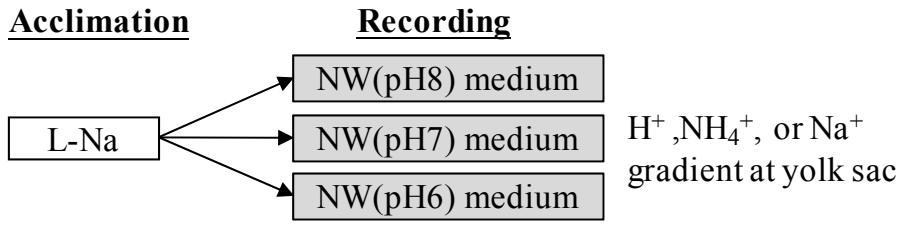

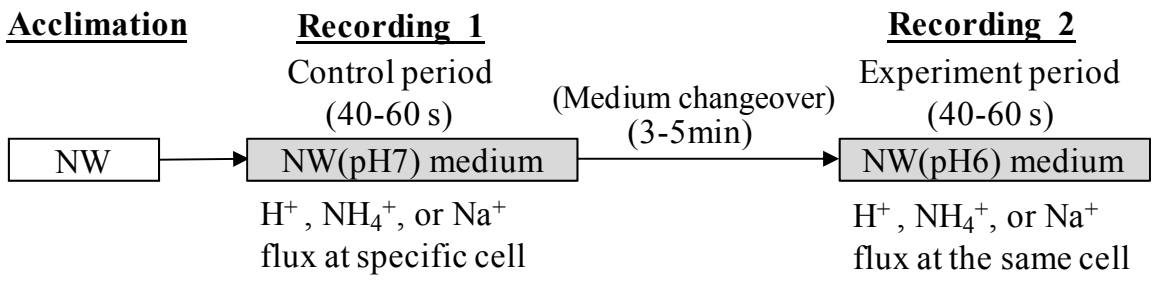

Results

Experiment 1.

Na^+, H^+, and NH_4^+ gradients at the skin of medaka larvae.

Surface ionic gradients of 7-dpf larvae acclimated to NW were measured with the SIET to determine the ionic excretion or uptake by larval skin. Seven spots on the surface of a larva were chosen for measurement: the snout, gills, pericardial cavity, yolk sac, trunk, cloaca, and tail (Fig. 1A). Figure 1B-D shows the ionic gradients at the seven spots by measuring the concentration difference between the target spot and the background (~10 mm away from the target spot). Results showed that $\Delta[H^+]$ and $\Delta[NH_4^+]$ were higher at the gills, pericardial cavity, and yolk sac than other spots, indicating that a larger excretion of H^+ and NH_4^+ occurred at these locations. However, $\Delta[Na^+]$ at the gills, pericardial cavity, and yolk sac were variable between individuals (Fig. 1D). Two of the four larvae measured showed negative values of $\Delta[Na^+]$ indicating net uptake of Na^+ by these larvae. However, the other two larvae showed net outflow of Na^+ at these locations.

Experiment 2.

Na^+, H^+, and NH_4^+ gradients in larvae acclimated to L-Na water.

Because the yolk sac surface showed notable gradients of H^+, NH_4^+, and Na^+, we choose this location to compare ionic gradients between NW- and L-Na-acclimated larvae (larvae were acclimated to L-Na for 5 days) (Fig. 2). Results showed that H^+ and NH_4^+ were excreted in NW larvae; however, Na^+ gradient was almost absent. L-Na acclimation remarkably increased Na^+ uptake (negative gradient of Na^+) and also increased NH_4^+ excretion (positive gradient

of NH_4^+). Notably, L-Na acclimation decreased the H^+ gradient indicating that H^+ secretion was suppressed or alkaline secretion was enhanced. In this experiment, no significant difference was found in mortality or hatching rates between the two groups.

Experiment 3.

Effects of EIPA on ionic gradients.

To test if the NHE is involved in Na^+ uptake and NH_4^+ excretion, an inhibitor (EIPA) was applied to the larvae by pre-immersion for 10 min. EIPA was not added to the recording media to prevent any alteration of the properties of the electrodes. $\Delta[H^+]$ at the larval skin was inhibited by around 28%, 22%, and 57% by 10, 100, and 1000 μM EIPA, respectively (Fig. 3A). The dosage of 1000 μM seemed too high for the larvae, since ~30% of the larvae were feeble or died after the treatment. Thus, we chose the dosage of 100 μM EIPA for the following experiments. L-Na-acclimated larvae which showed higher Na^+ and NH_4^+ gradients were used to test the effects of EIPA on Na^+ and NH_4^+ transport. Results showed that 100 μM EIPA significantly reduced NH_4^+ excretion by 35% (Fig. 3B) and Na^+ uptake by 54% ($\Delta[Na^+]$ decreased from -34±9 μM to -16±11 μM; Fig. 3C).

Experiment 4.

Na^+, H^+, and NH_4^+ fluxes at MRCs and KCs.

Under the microscope, MRCs in the skin could be identified by their oval shape and apical opening (membrane) (Fig. 4A). Using the SIET, ionic gradients at specific cells were determined by probing voltage differences of specific ions (Na^+, H^+, or NH_4^+) at 10-μm intervals perpendicular to the cell

membrane. Serial probing over the apical opening of MRCs and adjacent KCs is shown in Fig. 4A (the dashed line indicates a 40-μm probing route). The peak of voltage differences appeared right at the apical opening of MRCs, and the differences gradually decreased as the probe was moved away, revealing that MRCs are "hot spots" of Na^+ uptake and NH_4^+ excretion (Fig. 4C, D). Interestingly, contrary H^+ signals (H^+ sink and H^+ source) were found when probing over the MRCs, indicating that one group of MRCs secretes acid but another group secretes base (Fig. 4B). These two groups of MRCs were referred to as MRC^+ (acid-secreting) and MRC^- (base-secreting).

Experiment 5.

H^+, Na^+, and NH_4^+ fluxes at MRCs and KCs in larvae acclimated to L-Na or H-Amm.

L-Na acclimation was shown to decrease the H^+ gradient and increase the NH_4^+ gradient in the above experiment (Fig. 2). We further examined if the H^+ flux at MRCs and KCs was also affected by L-Na acclimation. Results showed that the H^+ flux at MRC^+ was about 16-fold higher than that at adjacent KCs in the normal group. L-Na acclimation significantly suppressed and reversed H^+ flux at KCs but did not significantly affect H^+ flux at either MRC^+ or MRC^- (Fig. 5A, B). However, the ratio of MRC^+ and MRC^- significantly changed. L-Na acclimation induced more MRC^- (Fig. 5D) and consequently decreased the H^+ gradient measured at the skin as shown in Fig. 2. The MRC^+/MRC^- ratio was calculated by pooling all recorded cells from different individuals. Fewer than 10 MRCs were usually recorded in the same individual.

To answer if the base secretion by MRCs is associated with NH_4^+ excretion, we examined larvae acclimated to H-Amm (5 mM NH_4^+). H-Amm acclimation

significantly decreased the number of MRC^+ and enhanced the number of MRC^- (Fig. 5D). Moreover, H^+ secretion was significantly suppressed at MRC^+, and the H^+ flux became more negative at KCs (Fig. 5A, C).

Since we were unable to discriminate between MRC^+ and MRC^- with a microscope, we only compared ungrouped MRCs and KCs in Na^+ and NH_4^+ fluxes. NH_4^+ fluxes at both KCs and MRCs were positive, which indicates excretion of NH_4^+ by these cells (Fig. 6A). By pooling all data together, 91% and 85% of the recorded MRCs (only MRCs with a clear opening) exhibited significant Na^+ uptake and NH_4^+ excretion (the fluxes were higher than those of KCs), respectively. The NH_4^+ flux at MRCs was about 11~13-fold higher than that at adjacent KCs in the three groups. Both L-Na and H-Amm acclimation induced NH_4^+ excretion at MRCs (Fig. 6A). Na^+ uptake (a negative Na^+ flux) was detected at MRCs in normal larvae; in contrast, outflow of Na^+ (a positive flux) was detected at KCs (Fig. 6B). Both L-Na and H-Amm acclimation significantly increased the Na^+ influx at MRCs by 60%. The outflow of Na^+ at KCs significantly decreased to nearly zero in L-Na and H-Amm larvae (Fig. 6B). Negligible background values (noise signals) recorded by probing in medium without larvae were 0.004±0.005, -0.03±0.62, and 2.8±5.1 pmole cm^{-2} s^{-1} (68, 24, and 37) using H^+, NH_4^+, and Na^+ electrodes, respectively.

Experiment 6.

Acute effects of external H-Amm on ionic gradients.

The above experiments showed a correlation between Na^+ uptake and NH_4^+ excretion. If NH_4^+ excretion can drive Na^+ uptake, a decrease in Na^+ uptake by blocking NH_4^+ excretion would be expected. In this experiment, we transferred larvae to the recording medium with H-Amm (2.5 mM $(NH_4)_2SO_4$)

and examined the effects of acute H-Amm exposure on the ionic gradients. Three groups of larvae which had been pre-acclimated to NW, L-Na, and H-Amm were compared. When measuring larvae in normal water, NH_4^+ excretion was higher in both the L-Na and H-Amm groups than in the NW group (Fig. 7A, black bars). Na^+ uptake was also higher in the L-Na and H-Amm groups (Fig. 7B, black bars). In contrast, the H^+ gradient was lower in the L-Na group and even decreased until it was negative in the H-Amm group (Fig. 7C, black bars). However, while measuring larvae in H-Amm water, dramatic changes occurred. External H-Amm reversed the NH_4^+ gradient from positive to negative values in the NW group, and decreased the NH_4^+ gradient to nearly zero in the L-Na and H-Amm groups (Fig. 7A, gray bars). Meanwhile, external H-Amm increased Na^+ outflow in the NW group and significantly blocked Na^+ uptake in the other two groups (Fig. 7B, gray bars). In contrast to changes in the NH_4^+ gradient, external H-Amm increased H^+ gradients in the three groups (Fig. 7C, gray bars).

Experiment 7.

Acute effects of external H-Amm on ionic fluxes at specific cells.

To answer if changes in the above experiment also take place in MRCs, we measured ionic fluxes at specific MRCs sequentially before and after H-Amm was applied. Figure 8A shows the Na^+ flux at three MRCs (closed symbols) and three KCs (open symbols) from different individuals. An inward Na^+ flux (Na^+ uptake) was recorded at MRCs before H-Amm exposure, but it was dramatically abolished or even reversed to an outward flux after H-Amm was applied (Fig. 8A, closed symbols). However, no significant change occurred at KCs (Fig. 8A, open symbols). Interestingly, we found that MRC^- turned into

MRC^+ after H-Amm was applied by sequentially probing the H^+ flux (Fig. 8B). Again, the KCs did not significantly change. H-Amm also suppressed NH_4^+ excretion at MRCs (Fig. 8C). It was also noticed that the NH_4^+ flux of cells became fluctuated after H-Amm was applied.

Experiment 8.

Acute effects of the external pH on ionic gradients and fluxes.

L-Na (pH 7)-acclimated larvae were measured in recording media with different pH values (pH 6, 7, and 8) to examine the effects of acute external pH change on ionic gradients. Acidic water (pH 6) significantly enhanced the NH_4^+ and Na^+ gradients but reversed the H^+ gradient at the larval skin (Fig. 9). However, alkaline water did not cause significant changes. Similar effects were also detected when probing ionic fluxes at specific MRCs. The H^+ flux at the three MRCs was positive but dramatically dropped to negative values when larvae were transferred from pH 7 to pH 6 water (Fig. 10A). Meanwhile, the Na^+ influx and NH_4^+ efflux at MRCs were also enhanced by the acidic water (Fig. 10B, C). However, the ionic fluxes at KCs (Fig. 10; open symbols) were relatively low and remained stable before and after the pH change.

Experiment 9.

External pH gradient at the apical surface of MRCs.

To reveal the H^+ gradient at the microenvironment above the apical surface of an MRC, serial SIET probing was performed starting from about 2 μm above the apical surface and gradually stepping away to > 100 μm (Fig. 11A; open circles). A parallel probing which began from the surface of a KC was also recorded for comparison (Fig. 11A; closed circles). In pH 6 water, the pH

detected exponentially dropped from 6.08 to 5.94 when probing 30 μm away from the MRC and remained relatively constant thereafter. The dropping of the pH revealed a microenvironment generated by base secretion (NH_3 excretion is suggested) of the MRC. Beyond the microenvironment, an acidic layer of ~100 μm thick was found. The acidic layer might be generated by acid secretion from KCs, since the pH measured at the KC was relatively constant and lower than the background pH. In addition, it was noted that the acidic layer was absent or unremarkable in yolk sac area when measuring the larvae in pH6 (data not shown). Therefore, the present data were recorded in trunk area adjacent to the yolk sac. As shown above (Fig. 9A, C), NH_4^+ excretion at the yolk sac was enhanced, and the H^+ gradient was simultaneously suppressed when probing the larvae in pH 6 water, suggesting that the enhanced NH_3 excretion consumed H^+ and diminished the acidic layer.

Discussion

By using a non-invasive electrophysiological technique, the SIET, this study provides direct and convincing evidence for Na^+ uptake and NH_4^+ excretion by MRCs in intact medaka larvae. As mentioned in the "Introduction", molecular evidence including localization of H^+-ATPase and the NHE in MRCs suggested that Na^+ uptake in FW fishes is mediated by MRCs. In addition, $^{22}Na^+$ uptake was found in a subtype of MRCs (PNA^-) using isolated branchial cells of rainbow trout (Reid et al., 2003). In zebrafish embryos, Na^+ accumulation was found in HRCs (a subtype of MRCs) using Sodium Green as an indicator (Esaki et al., 2007). Those recent studies suggested that MRCs are the major sites for Na^+ uptake in FW fishes. In this study, over 90% of the MRCs recorded (only MRCs in trunk skin with a clear apical opening were recorded) exhibited significant Na^+ uptake consolidating previous findings. In contrast to MRCs, Na^+ fluxes recorded at KCs were outward fluxes implying that Na^+ was lost passively from KCs. Active Na^+ uptake by MRCs apparently balanced the loss and thus made the Na^+ gradient at the skin surface very small. L-Na acclimation significantly induced compensatory Na^+ uptake at MRCs (Fig. 6B) which usually exhibited larger apical membranes (data not shown).

Interestingly, most MRCs recorded in medaka larvae also excreted a significant level of NH_4^+ suggesting that both Na^+ uptake and NH_4^+ excretion are conducted by the same MRCs. In zebrafish larvae, we found that NH_4^+ was highly excreted by HRCs (a subtype of MRCs) which also secrete a large amount of H^+ (Lin et al., 2006; Shih et al., 2008). Actually, we did not detect base-secreting MRCs in zebrafish. In medaka, although most MRCs excreted

NH_4^+, a large portion of MRCs (MRC^-) was found to secrete base instead of acid. These base-secreting MRCs seemed to be associated with Na^+ uptake and NH_4^+ excretion, since they could be induced by either L-Na or H-Amm acclimation (Fig. 5D). Precisely, the terms “acid-secreting” and “base-secreting” do not mean that a cell only secretes acid or base, but more acid or base. In the case of medaka, we suggest that MRC^- secretes more base than acid and thus it turns out to be a base-secreting cell.

So, what is the base secreted by MRCs? We suggest that non-ionic NH_3 is the dominant base which diffuses out of MRCs and titrates H^+ outside of MRCs. This acid-trapping mechanism for NH_3/NH_4^+ excretion was previously demonstrated in zebrafish (Shih et al., 2008). Our evidence presented in this study also supports this mechanism. NH_4^+ loading (H-Amm acclimation) increased the number of MRC^-, enhanced the NH_4^+ gradient, and also alkalized the skin surface (Fig. 7). In contrast, acutely transferring the larvae to H-Amm water suppressed NH_4^+ excretion and raised the H^+ gradient at the skin and also at individual MRCs (Figs. 7, 8). The reverse correlation between NH_4^+ and H^+ accumulation at the skin surface suggests that non-ionic NH_3 is excreted, and the more NH_3 which is excreted, the more H^+ outside that is titrated. In MRC^-, the amount of H^+ secreted is suggested to be less than that of non-ionic NH_3 secreted which caused an overall base-secretion. In contrast, MRC^+ may simply represent a lower NH_3-excreting and/or higher H^+-secreting cell. Interestingly, unpublished data from Hwang’s group showed that NHE3 (*slc9a3*) is highly expressed in a group of MRCs which does not have detectable H^+-ATPase (*atp6v1a*). In zebrafish, HRCs have both H^+-ATPase and NHE in the apical membrane (Yan et al., 2007). The differential expression of H^+-ATPase may explain why these two cases differ. In addition, we surprisingly found that the

NH_4^+ excretion by individual MRCs was much higher in medaka than in zebrafish (80 pmole cm^{-2} s^{-1} in the present study vs. 6 pmole cm^{-2} s^{-1} in Shih et al. 2008), suggesting a higher level of base (NH_3) secreted by MRCs of medaka than that of zebrafish.

Another major finding of this study is the tight linkage between Na^+ uptake and NH_4^+ excretion. EIPA at 100 μM inhibited both Na^+ uptake and NH_4^+excretion, although the levels were not the same. L-Na acclimation induced compensatory Na^+ uptake and also induced NH_4^+ excretion. Once again, H-Amm acclimation induced compensatory NH_4^+ excretion and also increased Na^+ uptake. Acutely raising the external NH_4^+ significantly blocked NH_4^+ excretion and Na^+ uptake. In contrast, acutely raising the acidity of water (pH 7 to pH 6) enhanced Na^+ uptake and NH_4^+ excretion. These data revealed a tight correlation between Na^+ uptake and NH_4^+ excretion not only by the SIET probing at the yolk sac skin but also at individual MRCs. This finding seems to support earlier studies which suggested Na^+/NH_4^+ exchange via NHE in fish gills (for review see Wilkie, 1997). However, we suggest that Na^+/NH_4^+ exchange is not simply mediated by the NHE. As mentioned in the "Introduction", early studies suggested that NH_4^+ may take the place of H^+ in the NHE and causes Na^+/NH_4^+ exchange; however, this suggestion has been argued in the previous study (Avella and Bornancin, 1989). If ionic NH_4^+ is transported by the NHE or other proteins such as Rh glycoproteins, alkalization of the surfaces of larval skin or MRCs should not occur. Our data apparently do not support this possibility. In addition, accumulating reports have suggested that Rh glycoproteins conduct non-ionic NH_3 instead of NH_4^+ (Nawata et al., 2007; Shih et al., 2008; Winkler, 2006). The identification of Rhbg and Rhcg mRNA in MRCs of medaka also supports the Rh proteins-dependent NH_3

excretion by acid-trapping (unpublished data). Taken together, we proposed a novel model to explain this Na^+/NH_4^+ exchange in the apical membrane of MRCs (Fig. 12). In this model, the two major players, NHE (NHE3 probably) and Rh glycoproteins (Rhbg and/or Rhcg), are functionally and probably physically associated. The Rh glycoprotein deprotonates NH_4^+ inside of MRCs and then facilitates non-ionic NH_3 diffusion down a chemical gradient generated by external acid-trapping mechanism. The H^+ dissociated from intracellular NH_4^+ may accumulate beneath the apical membrane and provides an effective H^+ gradient to drive Na^+ uptake via NHE3.

As mentioned in the "Introduction", the driving force of the NHE in gills of FW fishes has been debated for a long time (Parks et al., 2008). The present model provides a reasonable explanation for the driving force of the NHE and also for the Na^+/NH_4^+ exchange pathway. We also suggest that this model might not only work in medaka but also in other FW fishes. In zebrafish, Rhcg1 and NHE3 have been identified in the apical membrane of HRCs (Nakada et al., 2007a; Yan et al., 2007), and the mRNA of these two key players was found to be induced by L-Na acclimation (unpublished data). Pretreatment of apical L-Na water also induced mRNA expression of NHE2 and Rhcg2 in cultured branchial cells of rainbow trout (Tsui et al., 2009). These data suggest that NHE and Rh proteins are required for Na^+ uptake in FW fishes. In the special case of Osorezan dace which lives in an extremely acidic (pH 3.5) lake, NHE3 was located in the apical membrane of MRCs, and its mRNA expression in gills was higher in individuals reared in pH 3.5 than in individuals reared in pH 7 (Hirata et al., 2003). The NHE3 seems to be non-function in extremely acidic water, if considering the thermodynamics of the NHE. The authors suggested that Na^+/NH_4^+ exchange might be a possible

mechanism. It is quite possible that the dace also uses a mechanism similar to our model for Na^+ uptake.

External acidification is generally thought to suppress Na^+ uptake based on earlier studies on ion transport in frog skin. In 1949, Ussing proposed this notion for isolated frog skin, and Schoffeniels (1955) and Romeu et al. (1969) also found that Na^+ uptake was greatly suppressed as the skin external pH fell below 4 on *in vitro* or *in vivo* frog skin. Thereafter, several studies on goldfish (Maetz, 1973) and rainbow trout (Avella and Bornancin, 1989; Wright and Wood, 1985) also supported this finding. Current models for Na^+ uptake in apical membrane of MRCs including NHE- or H^+-ATPase-dependent pathway are basically derived from this early finding. However, several studies showed conflicting results. For example, external alkalization did not cause a higher Na^+ influx in rainbow trout (Wright and Wood, 1985); Na^+ influx was stimulated by external acidification and negatively correlated to water pH (Salama et al., 1999); Na^+ accumulation monitored by Sodium Green was stimulated by acidic water in HRCs of zebrafish embryos (Flynt et al., 2009). In the present study, increases in Na^+ uptake by yolk sac skin (Fig. 9B) and individual MRCs (Fig. 10B) were observed in medaka larvae transferred from pH 7 to pH 6. This finding seems against the NHE pathway for Na^+ uptake. However, comparing the H^+ flux and NH_4^+ flux before and after the acidic water transfer (Figs. 9, 10), once again a reverse correlation between the NH_4^+ and H^+ gradients suggests that an acid-trapping mechanism is involved. If non-ionic NH_3 excretion is associated with Na^+/H^+ exchange, acidic water-stimulating Na^+ uptake can reasonably be explained. Although the external low pH is theoretically unfavorable for Na^+ uptake via the NHE, in contrast, it is favorable for non-ionic NH_3 diffusion across apical membranes (Wilkie, 2002).

We suggest that external acid simultaneously promotes NH_3 excretion through Rh glycoproteins and intracellular H^+ accumulation (dissociated from NH_4^+) which in turn drives Na^+ uptake via the NHE.

In this study, a microenvironment above the opening of MRCs was shown by probing H^+ at serial points above the MRCs (Fig. 11). An acidic layer about 100 μm thick was detected surrounding the larva, and it gradually decayed with distance from the skin surface. The acidic layer is probably formed by H^+ secretion by MRC^+ or CO_2 diffusion from KCs. However, at the surface of the MRC, the pH dramatically increased when approaching the apical membrane of the MRC, showing this MRC to be a base-secreting MRC (MRC^-) in pH 6 water. The highest pH (6.08) was detected at a point ~2 μm away from the surface of apical membrane of the MRC. A higher pH may be 6.1 or more can be expected if the probe could get closer to the apical membrane. Base on this data, we still unable to determine if the H^+ gradient can drive Na^+ uptake, since intracellular or precisely the sub-apical pH is not available. This finding provides evidence for the existence of a microenvironment and the possibility of driving the NHE in fresh water. We suggest that a microenvironment with pH lower than cytosolic pH might exist on the other side of the apical membrane (intracellular). Future work using fluorescent pH indicators might be able to provide convincing evidence for the sub-apical microenvironment. However, we are still wondering if the determination of pH across apical membranes can answer the driving force for NHE. The pH gradient might be insignificant if the Rh glycoprotein and NHE have physical association or form a so called “metabolon” which has been found in bicarbonate transporters and carbonic anhydrase (Gross et al., 2002).

The molecular study on ion transport of medaka is relatively few at present

time. The proposed model apparently needs more molecular evidence to support. In the future, we may need to test our model by using loss-of-function or gain-of-function approaches such as gene knockdown or overexpresssion. In addition, the model may need to be tested in an *in vitro* system, such as the *Xenopus* oocyte expressing system. Moreover, several questions emerged in this study remain to be clarified. For instance, the function and mechanisms involved in MRC^+ is still unclear. We suggest that MRC^+ also take up Na^+ and excrete NH_4^+ but the involved mechanism may differ from that of MRC^-. Apical H^+-ATPase and putative ENaC may be involved in the function of MRC^+ and thus it makes MRC^+ to be an acid-secreting cell. This suggestion need to be tested in the future.

References

Avella, M. and Bornancin, M. (1989). A new analysis of ammonia and sodium transport through the gills of the freshwater rainbow trout (*Salmo gairdneri*). *J Exp Biol* **142**, 155-175.

Biver, S., Belge, H., Bourgeois, S., Van Vooren, P., Nowik, M., Scohy, S., Houillier, P., Szpirer, J., Szpirer, C., Wagner, C. A. et al. (2008). A role for Rhesus factor Rhcg in renal ammonium excretion and male fertility. *Nature* **456**, 339-43.

Boisen, A. M., Amstrup, J., Novak, I. and Grosell, M. (2003). Sodium and chloride transport in soft water and hard water acclimated zebrafish (*Danio rerio*). *Biochim Biophys Acta* **1618**, 207-18.

Braun, M. H., Steele, S. L., Ekker, M. and Perry, S. F. (2009). Nitrogen excretion in developing zebrafish (*Danio rerio*): a role for Rh proteins and urea transporters. *Am J Physiol Renal Physiol* **296**, F994-F1005.

Bury, N. R. and Wood, C. M. (1999). Mechanism of branchial apical silver uptake by rainbow trout is via the proton-coupled Na^+ channel. *Am J Physiol* **277**, R1385-91.

Choe, K. P., Kato, A., Hirose, S., Plata, C., Sindic, A., Romero, M. F., Claiborne, J. B. and Evans, D. H. (2005). NHE3 in an ancestral vertebrate: primary sequence, distribution, localization, and function in gills. *Am J Physiol Regul Integr Comp Physiol* **289**, R1520-34.

Donini, A. and O'Donnell, M. J. (2005). Analysis of Na^+, Cl^-, K^+, H^+ and NH_4^+ concentration gradients adjacent to the surface of anal papillae of the mosquito *Aedes aegypti*: application of self-referencing ion-selective microelectrodes. *J Exp Biol* **208**, 603-10.

Esaki, M., Hoshijima, K., Kobayashi, S., Fukuda, H., Kawakami, K. and Hirose, S. (2007). Visualization in zebrafish larvae of Na^+ uptake in mitochondria-rich cells whose differentiation is dependent on *foxi3a*. *Am J Physiol Regul Integr Comp Physiol* **292**, R470-80.

Evans, D. H., Piermarini, P. M. and Choe, K. P. (2005). The multifunctional fish gill: dominant site of gas exchange, osmoregulation, acid-base regulation, and excretion of nitrogenous waste. *Physiol Rev* **85**, 97-177.

Fenwick, J. C., Wendelaar Bonga, S. E. and Flik, G. (1999). *In vivo* bafilomycin-sensitive Na^+ uptake in young freshwater fish. *J Exp Biol* **202 Pt 24**, 3659-66.

Flynt, A. S., Thatcher, E. J., Burkewitz, K., Li, N., Liu, Y. and Patton, J. G. (2009). *miR*-8 microRNAs regulate the response to osmotic stress in zebrafish embryos. *J Cell Biol* **185**, 115-27.

Galvez, F., Reid, S. D., Hawkings, G. and Goss, G. G. (2002). Isolation and characterization of mitochondria-rich cell types from the gill of freshwater rainbow trout. *Am J Physiol Regul Integr Comp Physiol* **282**, R658-68.

Gross, E., Pushkin, A., Abuladze, N., Fedotoff, O. and Kurtz, I. (2002). Regulation of the sodium bicarbonate cotransporter kNBC1 function: role of Asp^{986}, Asp^{988} and kNBC1-carbonic anhydrase II binding. *J Physiol* **544**, 679-85.

Hirata, T., Kaneko, T., Ono, T., Nakazato, T., Furukawa, N., Hasegawa, S., Wakabayashi, S., Shigekawa, M., Chang, M. H., Romero, M. F. et al. (2003). Mechanism of acid adaptation of a fish living in a pH 3.5 lake. *Am J Physiol Regul Integr Comp Physiol* **284**, R1199-212.

Horng, J. L., Lin, L. Y., Huang, C. J., Katoh, F., Kaneko, T. and Hwang, P. P. (2007). Knockdown of V-ATPase subunit A (*atp6v1a*) impairs acid secretion and ion balance in zebrafish (*Danio rerio*). *Am J Physiol Regul Integr Comp Physiol* **292**, R2068-76.

Hung, C. Y., Tsui, K. N., Wilson, J. M., Nawata, C. M., Wood, C. M. and Wright, P. A. (2007). Rhesus glycoprotein gene expression in the mangrove killifish *Kryptolebias marmoratus* exposed to elevated environmental ammonia levels and air. *J Exp Biol* **210**, 2419-29.

Hwang, P. P. and Lee, T. H. (2007). New insights into fish ion regulation and mitochondrion-rich cells. *Comp Biochem Physiol A Mol Integr Physiol* **148**, 479-97.

Inokuchi, M., Hiroi, J., Watanabe, S., Lee, K. M. and Kaneko, T. (2008). Gene expression and morphological localization of NHE3, NCC and NKCC1a in branchial mitochondria-rich cells of Mozambique tilapia (*Oreochromis mossambicus*) acclimated to a wide range of salinities. *Comp Biochem Physiol A Mol Integr Physiol* **151**, 151-8.

Ivanis, G., Esbaugh, A. J. and Perry, S. F. (2008). Branchial expression and

localization of SLC9A2 and SLC9A3 sodium/hydrogen exchangers and their possible role in acid-base regulation in freshwater rainbow trout (*Oncorhynchus mykiss*). *J Exp Biol* **211**, 2467-77.

Kerstetter, T. H. and Keeler, M. (1976). On the interaction of NH_4^+ and Na^+ fluxes in the isolated trout gill. *J Exp Biol* **64**, 517-527.

Kerstetter, T. H., Kirschner, L. B. and Rafuse, D. D. (1970). On the mechanisms of sodium ion transport by the irrigated gills of rainbow trout (*Salmo gairdneri*). *J Gen Physiol* **56**, 342-359.

Khademi, S., O'Connell, J., 3rd, Remis, J., Robles-Colmenares, Y., Miercke, L. J. and Stroud, R. M. (2004). Mechanism of ammonia transport by Amt/MEP/Rh: structure of AmtB at 1.35 A. *Science* **305**, 1587-94.

Kirschner, L. B., Greenwald, L. and Kerstetter, T. H. (1973). Effect of amiloride on sodium transport across body surfaces of freshwater animals. *Am J Physiol* **224**, 832-837.

Krogh, A. (1939). *Osmotic Regulation in Aquatic Animals.* Cambridge: Cambridge University Press.

Lin, L. Y., Horng, J. L., Kunkel, J. G. and Hwang, P. P. (2006). Proton pump-rich cell secretes acid in skin of zebrafish larvae. *Am J Physiol Cell Physiol* **290**, C371-8.

Maetz, J. (1973). Na^+/NH_4^+, Na^+/H^+ exchanges and NH_3 movement across the gill of *Carassius Auratus*. *J Exp Biol* **58**, 255-275.

Maetz, J. and Garcia Romeu, F. (1964). The mechanism of sodium and chloride uptake by the gills of a fresh-water fish, *Carassius auratus*: II. evidence for NH_4^+/Na^+ and HCO_3^-/Cl^- exchanges. *J Gen Physiol* **47**, 1209-1227.

McDonald, D. G. and Millsgan, C. L. (1988). Sodium transport in the brook trout, *Salvelinus fontinalis*: effects of prolonged low pH exposure in the presence and absence of aluminum. *Can J Fish Aquat Sci* **45**, 1606-1613.

Nakada, T., Hoshijima, K., Esaki, M., Nagayoshi, S., Kawakami, K. and Hirose, S. (2007a). Localization of ammonia transporter Rhcg1 in mitochondrion-rich cells of yolk sac, gill, and kidney of zebrafish and its ionic strength-dependent expression. *Am J Physiol Regul Integr Comp*

Physiol **293**, R1743-53.

Nakada, T., Westhoff, C. M., Kato, A. and Hirose, S. (2007b). Ammonia secretion from fish gill depends on a set of Rh glycoproteins. *FASEB J* **21**, 1067-74.

Nawata, C. M., Hung, C. C., Tsui, T. K., Wilson, J. M., Wright, P. A. and Wood, C. M. (2007). Ammonia excretion in rainbow trout (*Oncorhynchus mykiss*): evidence for Rh glycoprotein and H^+-ATPase involvement. *Physiol Genomics* **31**, 463-74.

Parks, S. K., Tresguerres, M. and Goss, G. G. (2007). Interactions between Na^+ channels and Na^+-HCO_3^- cotransporters in the freshwater fish gill MR cell: a model for transepithelial Na^+ uptake. *Am J Physiol Cell Physiol* **292**, C935-44.

Parks, S. K., Tresguerres, M. and Goss, G. G. (2008). Theoretical considerations underlying Na^+ uptake mechanisms in freshwater fishes. *Comp Biochem Physiol C Toxicol Pharmacol* **148**, 411-8.

Payan, P. (1978). A study of the Na^+/NH_4^+ exchange across the gill of the perfused head of the trout (*Salmo gairdneri*). *J Comp Physiol B* **124**, 181-188.

Randall, D. J., Burggren, W. W. and French, K. (2002). Eckert Animal Physiology: Mechanisms and Adaptations. 5th edition. *Freeman, NY, USA.*, 588-620.

Randall, D. J., Wilson, J. M., Peng, K. W., Kok, T. W., Kuah, S. S., Chew, S. F., Lam, T. J. and Ip, Y. K. (1999). The mudskipper, *Periophthalmodon schlosseri*, actively transports NH_4^+ against a concentration gradient. *Am J Physiol* **277**, R1562-7.

Reid, S. D., Hawkings, G. S., Galvez, F. and Goss, G. G. (2003). Localization and characterization of phenamil-sensitive Na^+ influx in isolated rainbow trout gill epithelial cells. *J Exp Biol* **206**, 551-9.

Romeu, F. G., Salibian, A. and Pezzani-Hernandez, S. (1969). The nature of the *in vivo* sodium and chloride uptake mechanisms through the epithelium of the Chilean frog *Calyptocephalella gayi* (Dum. et Bibr., 1841): exchanges of hydrogen against sodium and of bicarbonate against chloride. *J Gen Physiol* **53**, 816-835.

Salama, A., Morgan, I. J. and Wood, C. M. (1999). The linkage between Na^+ uptake and ammonia excretion in rainbow trout: kinetic analysis, the effects of $(NH_4)_2SO_4$ and NH_4HCO_3 infusion and the influence of gill boundary layer pH. *J Exp Biol* **202 (Pt 6)**, 697-709.

Schoffeniels, E. (1955). Influence du pH sur le transport actif de sodium a travers la peau de grenouille. *Archs Int Physiol Biochim* **63**, 513-530.

Shaw, J. (1960). The absorption of sodium ions by the crayfish *Astacus pallipes* lereboullet: III. the effect of other cations in the external solution. *J Exp Biol* **37**, 548-556.

Shih, T. H., Horng, J. L., Hwang, P. P. and Lin, L. Y. (2008). Ammonia excretion by the skin of zebrafish (*Danio rerio*) larvae. *Am J Physiol Cell Physiol* **295**, C1625-32.

Smith, P. J., Hammar, K., Porterfield, D. M., Sanger, R. H. and Trimarchi, J. R. (1999). Self-referencing, non-invasive, ion selective electrode for single cell detection of trans-plasma membrane calcium flux. *Microsc Res Tech* **46**, 398-417.

Tsui, T. K., Hung, C. Y., Nawata, C. M., Wilson, J. M., Wright, P. A. and Wood, C. M. (2009). Ammonia transport in cultured gill epithelium of freshwater rainbow trout: the importance of Rhesus glycoproteins and the presence of an apical Na^+/NH_4^+ exchange complex. *J Exp Biol* **212**, 878-92.

Wilkie, M. P. (1997). Mechanisms of ammonia excretion across fish gills. *Comp Biochem Physiol A Mol Integr Physiol* **118**, 39-50.

Wilkie, M. P. (2002). Ammonia excretion and urea handling by fish gills: present understanding and future research challenges. *J Exp Zool* **293**, 284-301.

Wilkie, M. P. and Wood, C. M. (1994). The effects of extremely alkaline water (pH 9.5) on rainbow trout gill function and morphology. *J Fish Biol* **45**, 87-98.

Wilson, J. M., Laurent, P., Tufts, B. L., Benos, D. J., Donowitz, M., Vogl, A. W. and Randall, D. J. (2000). NaCl uptake by the branchial epithelium in freshwater teleost fish: an immunological approach to ion-transport protein localization. *J Exp Biol* **203**, 2279-96.

Wilson, R. W., Wright, P. M., Munger, S. and Wood, C. M. (1994). Ammonia excretion in freshwater rainbow trout (*Oncorhynchus mykiss*) and the importance of gill boundary layer acidification: lack of evidence for Na^+/NH_4^+ exchange. *J Exp Biol* **191**, 37-58.

Winkler, F. K. (2006). Amt/MEP/Rh proteins conduct ammonia. *Pflugers Arch* **451**, 701-7.

Wright, P. A., Randall, D. J. and Perry, S. F. (1989). Fish gill water boundary layer: a site of linkage between carbon dioxide and ammonia excretion. *J Comp Physiol B* **158**, 627-635.

Wright, P. A. and Wood, C. M. (1985). An analysis of branchial ammonia excretion in the freshwater rainbow trout: effects of environmental pH change and sodium uptake blockade. *J Exp Biol* **114**, 329-353.

Yan, J. J., Chou, M. Y., Kaneko, T. and Hwang, P. P. (2007). Gene expression of Na^+/H^+ exchanger in zebrafish H^+ -ATPase-rich cells during acclimation to low-Na^+ and acidic environments. *Am J Physiol Cell Physiol* **293**, C1814-23.

Figures

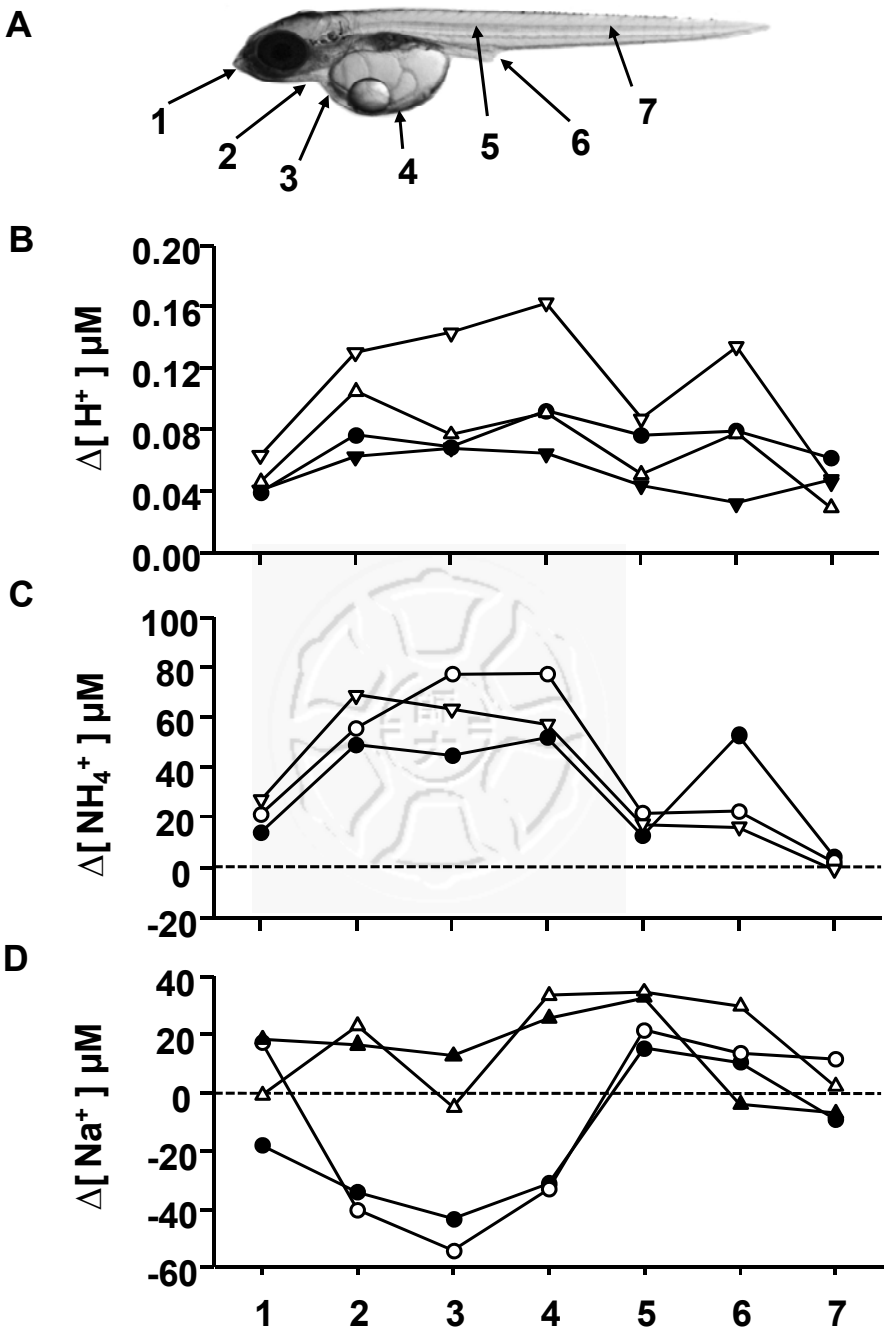

Fig. 1. Ionic gradients ($\Delta[H^+]$, $\Delta[NH_4^+]$, and $\Delta[Na^+]$) at the skin surface of medaka larvae. A: the seven spots measured with the scanning ion-selective electrode technique (SIET): snout (1), gill (2), pericardial cavity (3), yolk sac (4), trunk (5), cloaca (6), and tail (7). Each line in B~D represents the ionic gradients at the seven spots on different individuals.

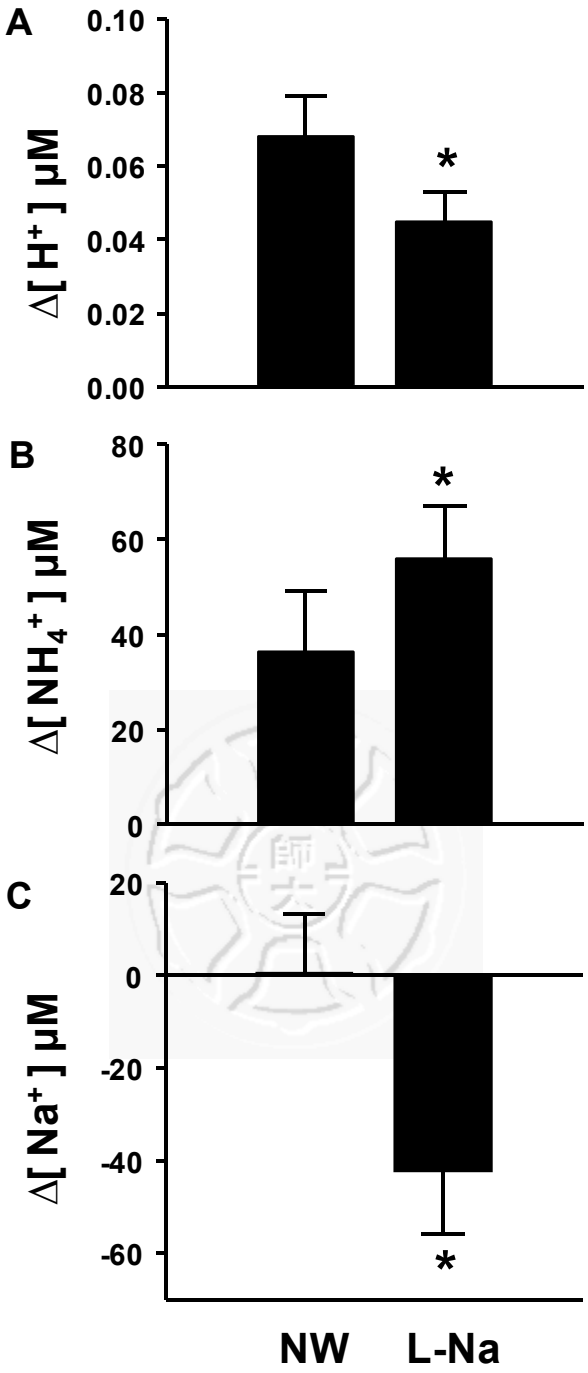

Fig. 2. Ionic gradients ($\Delta[H^+]$, $\Delta[NH_4^+]$, and $\Delta[Na^+]$) at the yolk sac surface of larvae acclimated to normal water (NW) or low Na^+ water (L-Na). Data are presented as the mean ± SD (n = 10). *Significant difference between the NW and L-Na groups (Student's t-test, $p < 0.05$).

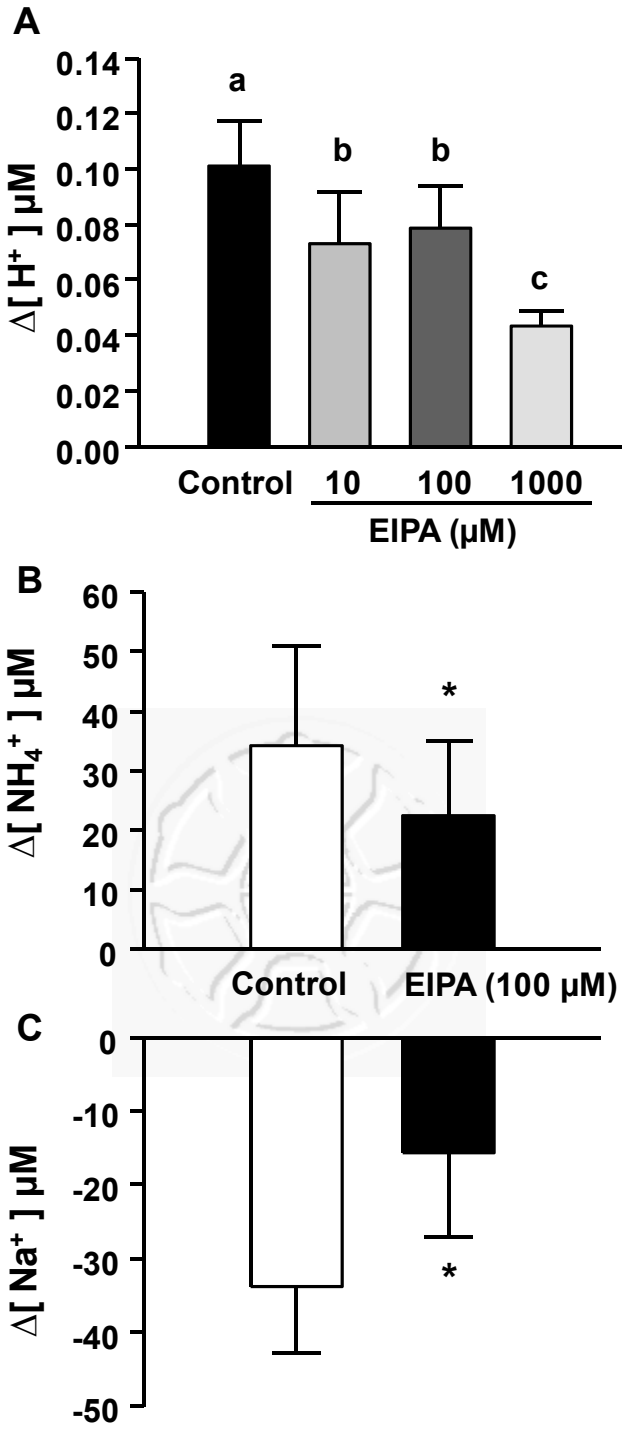

Fig. 3. A: Effects of EIPA (10~1000 μM) on $\Delta[H^+]$ at the yolk sac surface of 7-day post-fertilization (dpf) normal water (NW) larvae. B and C: Effects of 100 μM EIPA on $\Delta[NH_4^+]$ and $\Delta[Na^+]$ at the yolk sac surface of low-Na^+ water (L-Na)-acclimated larvae. Data are presented as the mean ± SD (n = 10). Different letters indicate a significant difference (one-way ANOVA, Tukey's comparison, $p < 0.05$). *Significant difference (Student's t-test, $p < 0.05$).

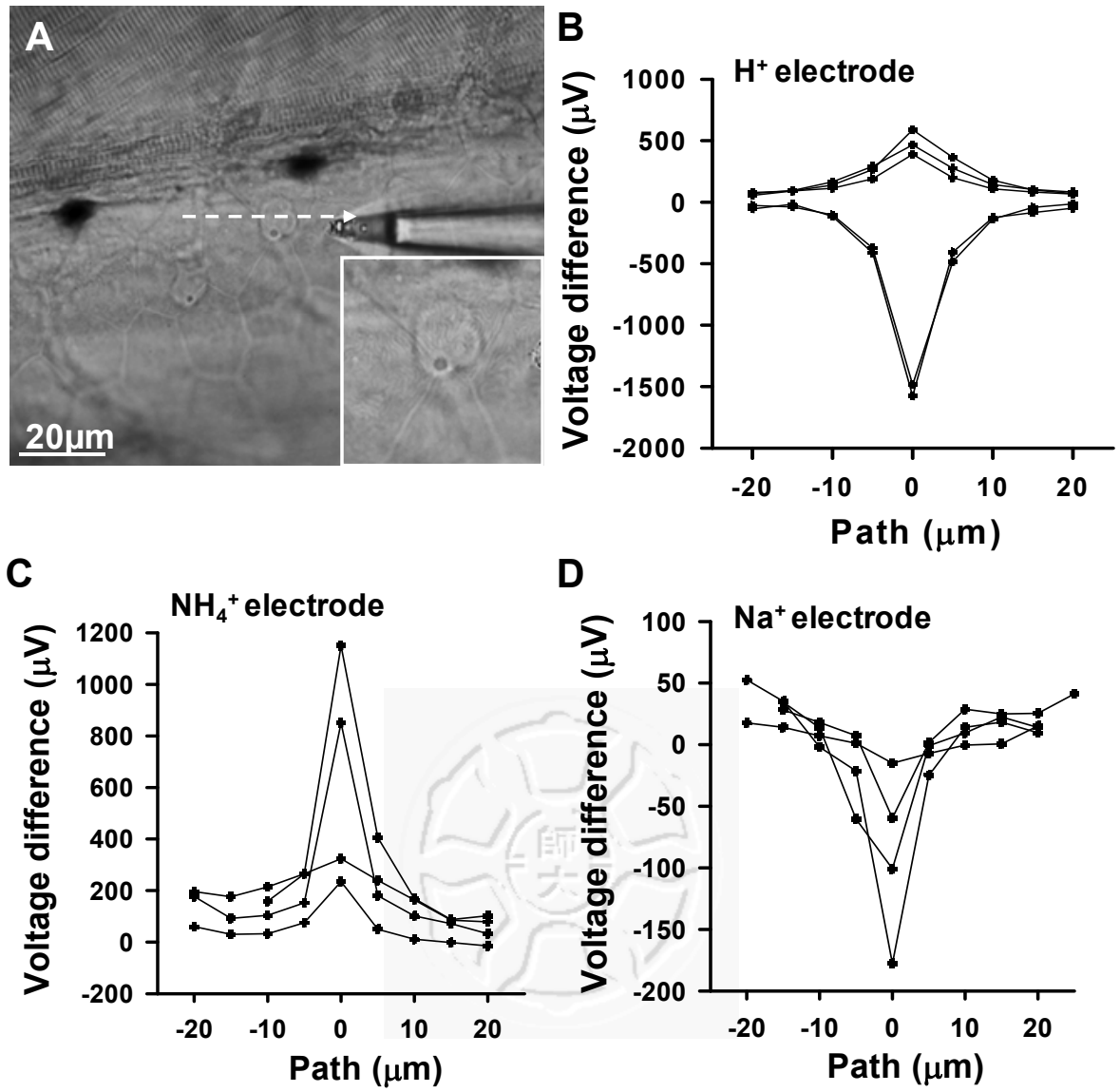

Fig. 4. Scanning ion-selective electrode technique (SIET) probing at specific cells on the skin of medaka larvae. A: Under the microscope, the apical membranes of mitochondria-rich cells (MRCs) was identified, and a "line scan" was performed by probing at a series of locations along a line (arrow) across the surface of the MRCs and adjacent keratinocytes (KCs). B-D: Voltage differences of the SIET probing with H^+-, NH_4^+-, or Na^+-selective microelectrodes, respectively.

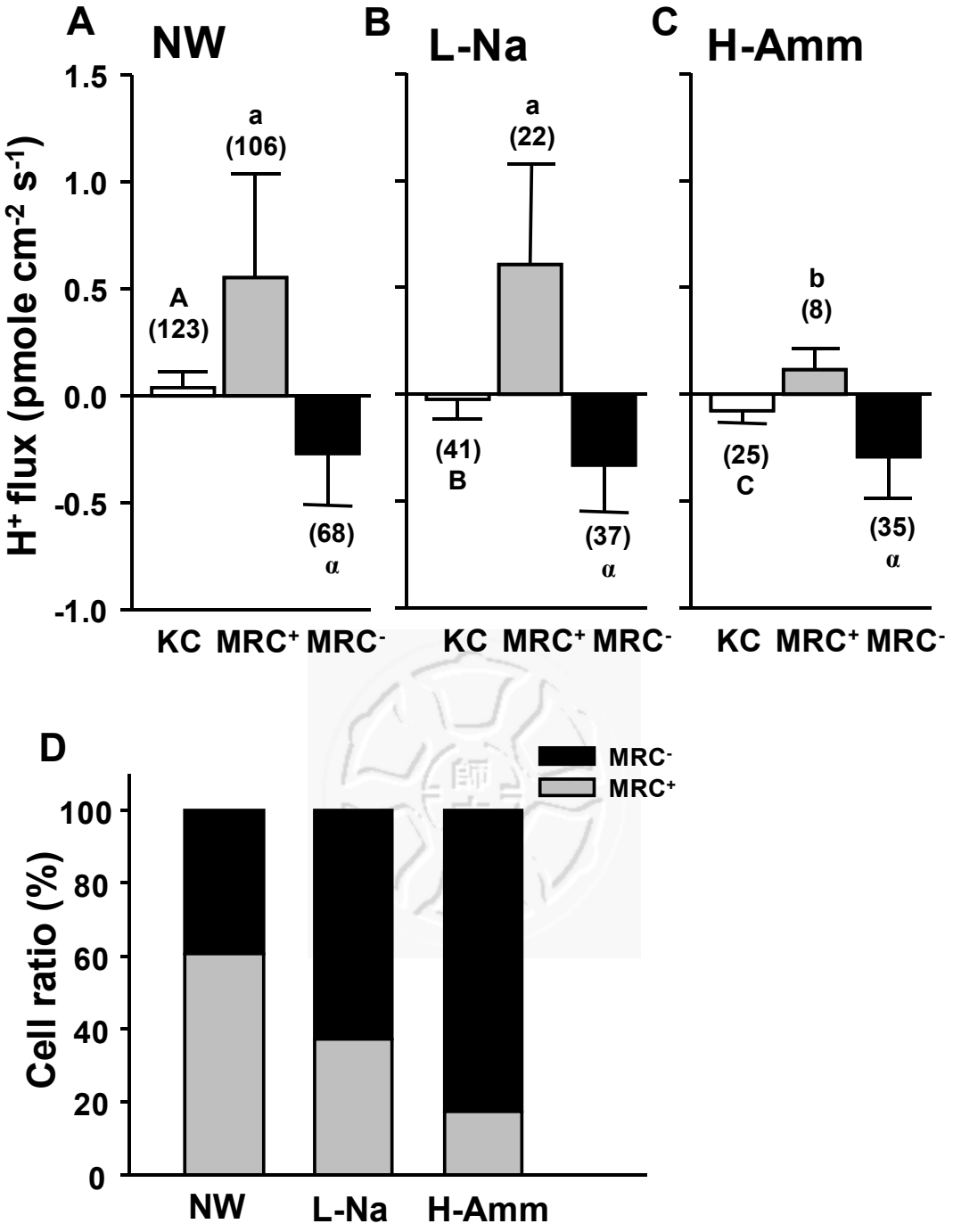

Fig. 5. A: H^+ fluxes at mitochondira-rich cells (MRCs) and keratinocytes (KCs) on the skin of medaka larvae acclimated to normal water (NW), low-Na^+ water (L-Na), or high-NH_4^+ water (H-Amm). Based on the direction of the H^+ flux, MRCs were grouped into MRC^+ (acid-secreting MRCs) and MRC^- (base-secreting MRCs). B: Ratio of MRC^+ and MRC^- recorded from different individuals. Data are presented as the mean ± SD (*n*). Different letters indicate a significant difference (one-way ANOVA, Tukey's comparison, $p < 0.05$).

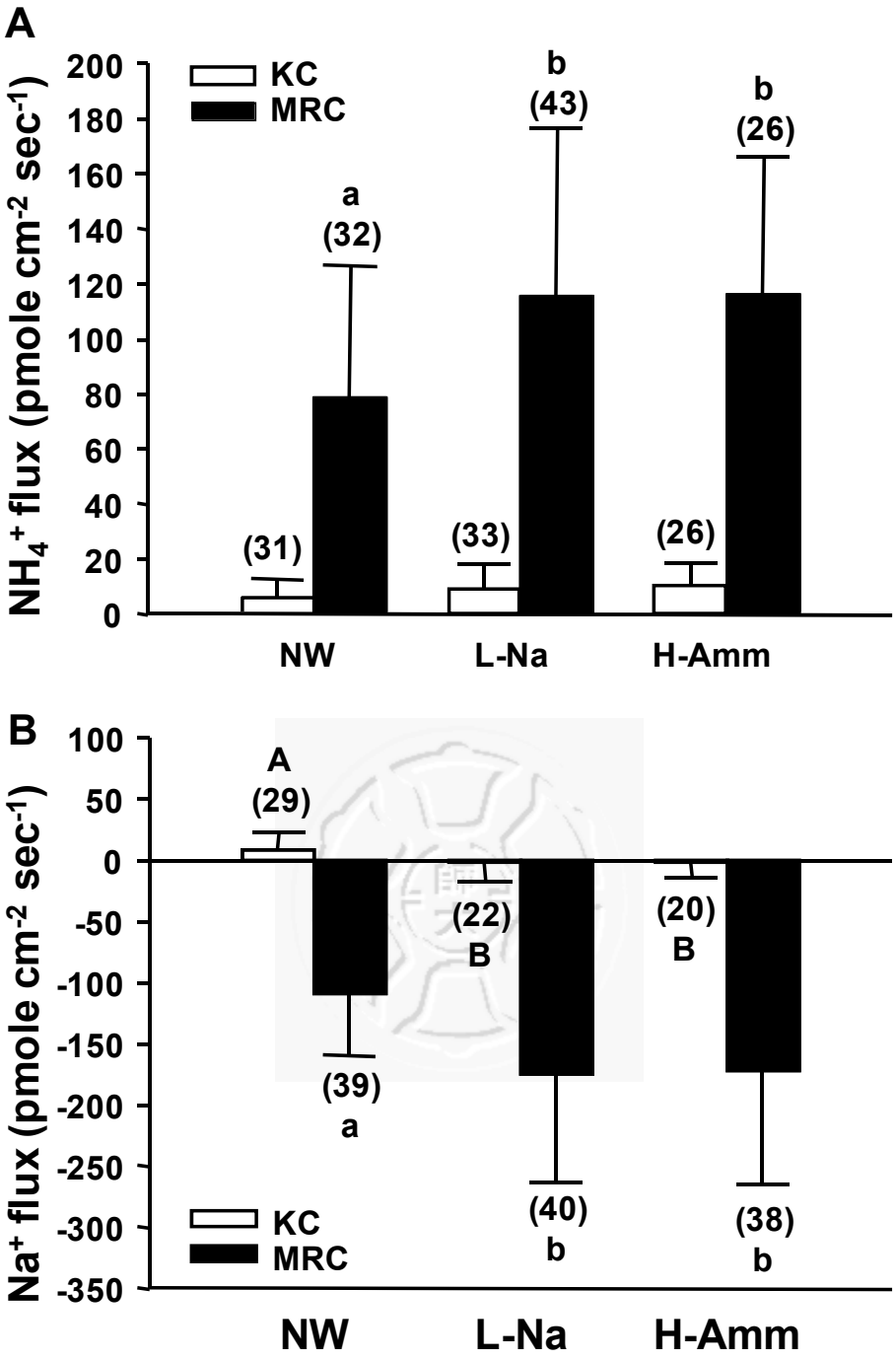

Fig. 6. NH_4^+ fluxes (A) and Na^+ fluxes (B) at mitochondira-rich cells (MRCs) and keratinocytes (KCs) on the skin of medaka larvae acclimated to normal water (NW), low-Na^+ water (L-Na), or high-NH_4^+ water (H-Amm). Data are presented as the mean ± SD (*n*). Different letters indicate a significant difference (one-way ANOVA, Tukey's comparison, $p < 0.05$).

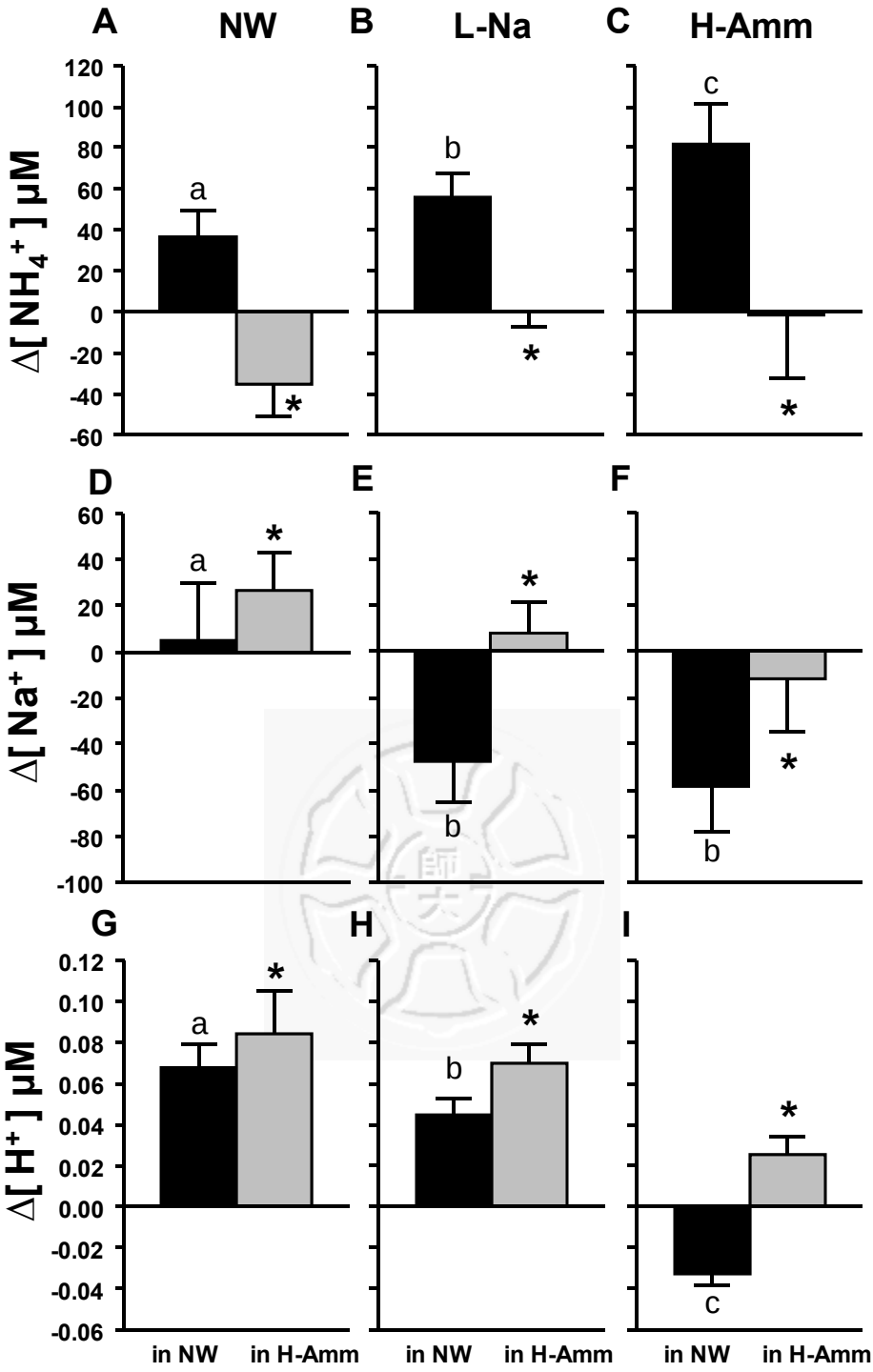

Fig. 7. Acute effects of external high-NH_4^+ water (H-Amm) (5 mM NH_4^+) on $\Delta[NH_4^+]$ (A-C), $\Delta[Na^+]$ (D-F), and $\Delta[H^+]$ (G-I) at the yolk sac surface of larvae acclimated to normal water (NW), low-Na^+ water (L-Na), or H-Amm. After acclimation, the larvae were measured in NW medium (black bars) or H-Amm medium (gray bars). Data are presented as the mean ± SD (n = 10). Different letters indicate a significant difference among the three acclimation groups (one-way ANOVA, Tukey's comparison, $p < 0.05$). *Significant difference between the two groups measured in H-Amm or in NW (Student's t-test, $p < 0.05$).

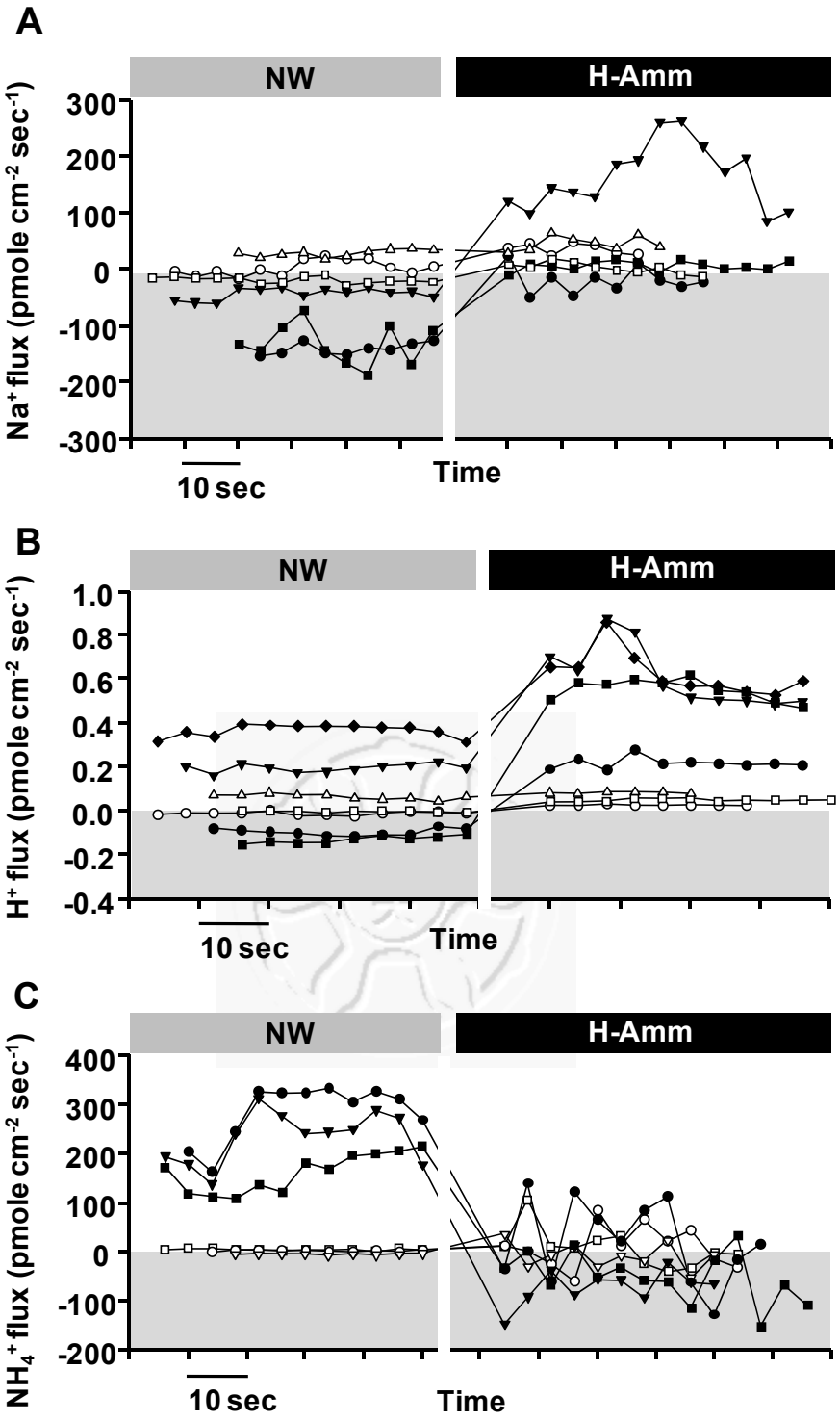

Fig. 8. Acute responses of mitochondria-rich cells (MRCs) and keratinocytes (KCs) to external high-NH_4^+ water (H-Amm) (5 mM NH_4^+). Ionic fluxes were recorded sequentially before and after H-Amm exposure at MRCs and KCs. Each line represents the sequential fluxes of an MRC (closed symbols) or a KC (open symbols). The gray bar and black bars represent normal water (NW) medium and H-Amm medium respectively. The break of time indicates a 3~5-min duration for changing the medium.

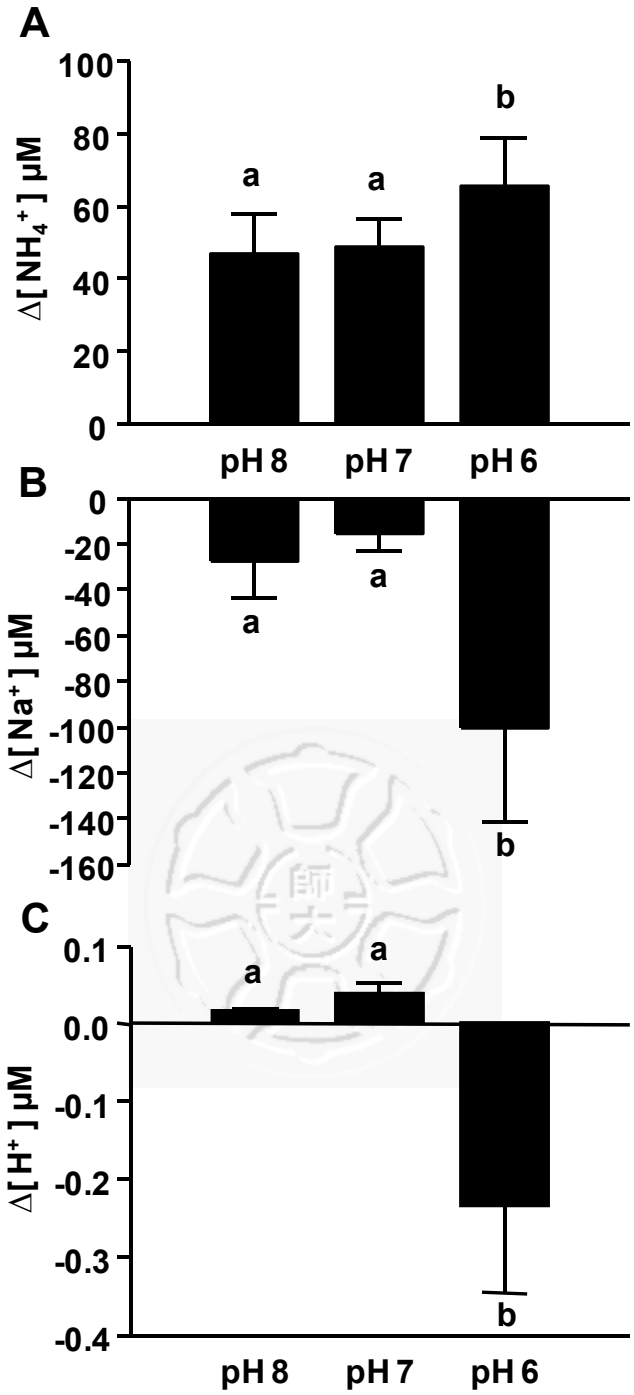

Fig. 9. Effects of pH changes on $\Delta[NH_4^+]$ (A), $\Delta[Na^+]$ (B), and $\Delta[H^+]$ (C) at the yolk sac surface of larvae acclimated to low-Na^+ water (L-Na). Larvae were acclimated to L-Na (pH 7) to enhance Na^+ uptake and then recorded in different pH waters (pH6, 7, or 8). Data are presented as the mean ± SD (n = 10). Different letters indicate a significant difference (one-way ANOVA, Tukey's comparison, $p < 0.05$).

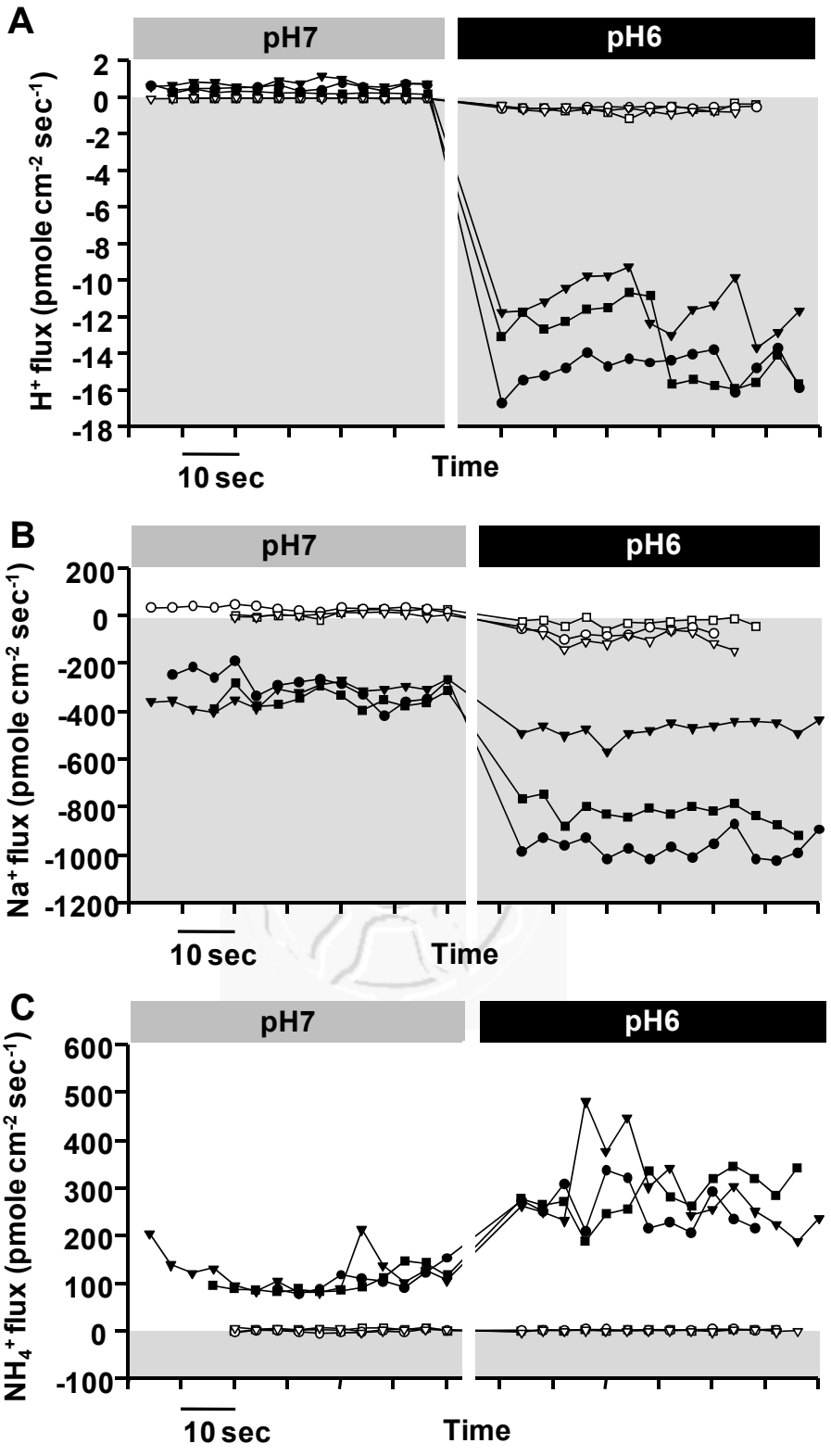

Fig. 10. Acute responses of mitochondria-rich cells (MRCs) and keratinocytes (KCs) to acidic water. Each line represents the sequential fluxes of an MRC (closed symbols) or a KC (open symbols). The gray bar and black bars represent pH 7 medium and pH 6 medium respectively. The break of time indicates a 3~5-min duration for changing the medium.

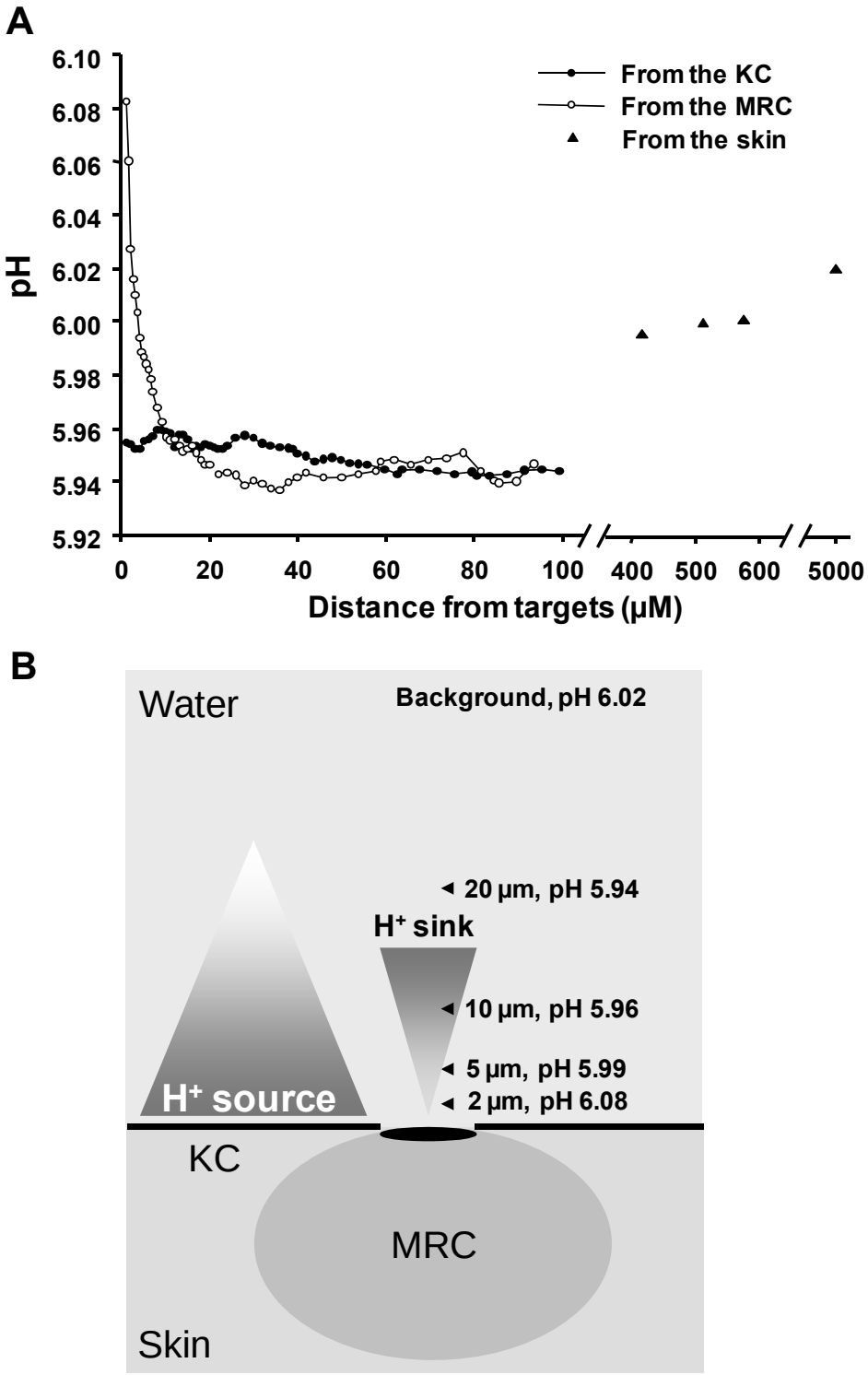

Fig. 11. Spatial changes in pH in the microenvironment generated by a mitochondria-rich cell (MRC) on the skin of medaka larvae. An egress recording of pH was performed by a serial scanning ion-selective electrode technique (SIET) probing from the apical membrane (about 2 μm from the surface of the membrane) of an MRC (open symbols) or an adjacent keratinocyte (KC) (closed symbols) to the background (5000 μm away from the skin). The larva was measured in pH 6 medium and the recorded background pH was about 6.02.

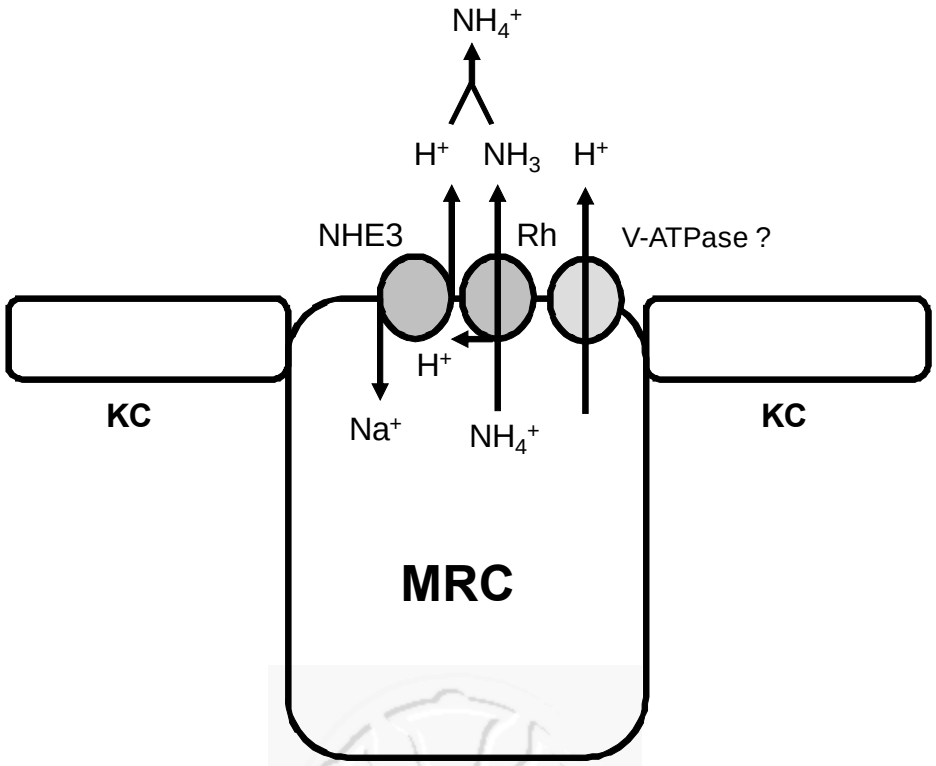

Fig. 12. Proposed model of "NH_4^+-dependent Na^+ uptake" in mitochondria-rich cells (MRCs) of medaka larvae. The two key players, the Na^+/H^+ exchanger (NHE) and Rhesus glycoprotein (Rh) are suggested to be involved in the apical transport of Na^+ and NH_4^+. The Rh deprotonates NH_4^+ inside the apical membrane and facilitates NH_3 gas diffusion down the gradient generated by "the acid-trapping of NH_3" outside of the membrane. Rh-mediated NH_4^+ excretion may generate an H^+ gradient across the apical membrane to drive Na^+ uptake through the NHE.